 doi:10.20944/preprints201807.0226.v1

Recent Advances in Nanoparticle Shape and Composition Regulation Based on Galvanic Replacement for Cancer Treatment

Woojun Shin[a‡], Kyungtae Kang[b‡] and Hongje Jang[a*]

[a]Department of Chemistry, Kwangwoon University, 20 Gwangwoon-ro, Nowon-gu, Seoul 01897, Republic of Korea

[b]Department of Applied Chemistry, Kyung Hee University, Yongin, Gyeonggi 446-701, Republic of Korea

Abstract

Owing to their unique physicochemical properties, nanoparticles are used in a variety of ways in the field of cancer treatment, including imaging, drug delivery, and photothermal and photodynamic therapies. The fascinating properties of nanoparticles are determined by their size, morphology, and constituent elements, and various synthetic methods and post-synthetic techniques have been applied to control these factors. Herein, we present examples of shape and composition control through galvanic replacement, a technique that exploits redox potential differences between elements to induce spontaneous ion-exchange and highlight its specific contributions to cancer treatment applications. The present article identifies the recent advances in nanoparticle formation techniques and discusses the future outlook of the field.

1. Introduction

Cancer is regarded as one of the most critical diseases because of the few early signs and metastasis to other organs. Therefore, its prevention and early diagnosis are very important academically, socially, and economically [1-7]. Unfortunately, cancer has a poor prognosis and it is difficult to diagnose early, except through regular health checkups [8-12]. Thus, effective and successful treatment of cancer has long been established as a more practical and essential research field. As conventional cancer treatments, surgery and chemotherapy are the most representative and widely used treatment strategies. In the case of surgery, effective treatment, even for mid-

Preprints (www.preprints.org) | NOT PEER-REVIEWED | Posted: 13 July 2018 doi:10.20944/preprints201807.0226.v1

and late-stage cancer, is possible through cancer tissue extraction, but this strategy presents numerous drawbacks, including its very invasive nature and the risks during surgery [13]. Chemotherapy can also be used in conjunction with surgery or long-term medication, but the high cost, severe side effects of anticancer drugs, and sequelae are problematic [14-16]. Accordingly, several new cancer therapies have been developed, including controlled drug delivery [17-20], photothermal therapy [21-24], and photodynamic therapy [25-28], and these strategies are attracting considerable attention as promising cancer therapies.

These next-generation cancer treatment techniques are being implemented using various nanoparticles to maximize the treatment efficiencies. The term "nanoparticles" generally refers to small metal or non-metallic objects with diameters in the 1–1000 nm range [29,30]; diameters within 200 nm are generally required for biomedical applications such as drug delivery and photoinduced therapies [31-35]. Such nanometer-scale materials exhibit physicochemical properties that are very different from those exhibited by everyday materials. For example, Au is a glossy metallic substance as a bulk material, but Au nanoparticles have various colors owing to surface plasmon resonance [36,37] caused by the quantum confinement effect [38-40]. Numerous studies have been performed in the field of cancer treatment using nanoparticles because of the dependence of their unique characteristics and efficiencies on their shape [41-45], size [46-50], and composition [51-54]. Among them, Au nanoparticles have been established as the most effective and promising nanomaterials for many decades owing to factors such as biocompatibility [55-60], colloidal stability [61-64], and drug loading capacity [65-67], which are essential criteria for therapeutic applications.

In this review, we introduce recent research trends and achievements in the regulation of nanoparticle shape and composition, which present new possibilities in nanoparticle-based cancer treatments that depend on nanoparticles of definite compositions and shapes.

2. Galvanic replacement

Galvanic replacement, first reported by Xia's group in 2003, involves spontaneous metal element exchange reactions between sacrificial nanoparticle templates with lower standard reduction potentials and metal cations with higher standard reduction potentials [68]. Generally, Ag [69-85], Cu [86-91], and Ni [92-95] are used as template nanoparticles, and Au, Pt, and Pd are used as replacing cations by selecting the appropriate reduction potential difference. During the galvanic replacement reaction, the replacing metal cation approaches the template

Preprints (www.preprints.org) | NOT PEER-REVIEWED | Posted: 13 July 2018 doi:10.20944/preprints201807.0226.v1

surface and triggers a spontaneous redox reaction to achieve reduction and deposition on the external surface of the template. As a counter reaction, the template elements are oxidized and dissolved into solution maintaining stoichiometric electron balance. Since core-shell or hollow nanoshell structures can be selectively synthesized by exploiting the stoichiometric electron balance, galvanic replacement is regarded as suitable for the formation of specific three-dimensional (3D) nanostructures [96-103]. However, there are some drawbacks to conventional galvanic replacement. First, excessive replacement causes fragmentation or aggregation because of uncontrollable replacement after the formation of a nanoshell [104,105]. Second, insoluble byproducts such as AgCl are formed by the dissolved template element (Ag^+), and the counter ion of the replacing cation (Cl^-) is deposited on the surface of the particles, reducing colloidal stability [106-108]. Recently, research into galvanic-replacement-mediated nanostructure formation has been performed extensively in order to overcome these shortcomings and increase the pool of applicable elements.

2.1. Conventional shape control by galvanic replacement

Since the development of galvanic replacement, its most common application has been the formation of hollow nanocages with interior vacancies. Hollow nanocages exhibit fascinating characteristics, in that their localized surface plasmon resonances (LSPRs) shift to the near-infrared (NIR) wavelength region owing to the narrowing of the energy gap between the anti-symmetric anti-bonding resonance modes and the symmetric bonding resonance modes depending on shell thickness and diameter [109-118]. These high-extinction features in the NIR region induce strong exothermic phenomenon caused by the surface plasmon oscillation through laser irradiation in the corresponding wavelength range, which is often referred to as photothermal conversion [119-133]. In cancer treatment, photothermal conversion is highly efficient in killing cancer cells vulnerable to hyperthermia. Furthermore, the NIR-region absorbance endowed by the hollow nanocage structures corresponds to the photothermal therapeutic wavelength window, which does not overlap with the light absorbing region of substances in the body such as hemoglobin, fat, and water. Since the tissue penetration of NIR light is superior to that of visible light and ultraviolet rays, it presents huge advantages when combined with hollow nanoparticles [134-143].

2.1.1. Hollow nanoshells

Preprints (www.preprints.org) | NOT PEER-REVIEWED | Posted: 13 July 2018 doi:10.20944/preprints201807.0226.v1

To maximize NIR absorption characteristics, template nanoparticle morphology control has been achieved to obtain hollow nanoshells of various shapes. Since the first report of Au nanocages synthesized from Ag nanocubes, various hollow Au nanoshell structures have been prepared using Ag nanospheres [144-155], Ag nanorods [156-159], Ag nanowires [160], and even Ag islands on two-dimensional surfaces as templates [161]. The LSPR red-shift due to the formation of a hollow nanostructure leads to efficient photothermal conversion under laser irradiation, which is observed to be excellent for all these hollow structures. By applying the same galvanic replacement method to different templates, hollow nanocages, hollow nanoshells, hollow nanorods, hollow nanowires, and even hollow dendritic structures can be obtained very easily. Furthermore, this technique is not limited to Au. Of course, hollow Au nanostructures are used for various biomedical applications including cancer treatment because of their high biocompatibility and excellent LSPR efficiencies, but it can also be applied to Pt [162-166] and Pd [167-170], which have higher reduction potentials than the template Ag. In addition to these widely used photothermal therapies, bioconjugation and optical contrast agents for bioimaging have been studied as applications of hollow Au nanostructures. Along with the primary formation of simple hollow nanoshells, various post-synthetic processing techniques have been developed to improve optical efficiency and control the absorption wavelength range, making it more suitable for use. One of the most interesting approaches is the formation of hollow multi-shell structures through repetitive galvanic replacement using the preferentially formed hollow nanoshell itself as a secondary template, rather than simply controlling the size or thickness of the nanoshell. The surface of the formed initial structure is coated with an Ag shell through reduction of Ag cations by a reducing agent, and then galvanic replacement is performed to form a hollow nanoshell [171]. This process can be repeated as many times as desired to form a multi-shell structure, and additional LSPR shifting with optical density enhancement can be achieved based on the difference in electron distribution inside and outside the nanoshell. Thus, more optical efficiency can be expected from the same number of particles. Furthermore, such multi-shell structures exhibit high applicability. However, relatively few practical studies on such systems have been conducted due to the inconvenience of repeated syntheses and purification.

2.1.2. Nanoframes

A nanoframe is a type of skeletal nanostructure based on galvanic replacement and is often distinguished from hollow nanostructures. This category includes not only 3D skeletal nanostructures that are structurally similar to nanocages but also annular planar nanostructures. Planar nanoframe structures that are distinct from the

Preprints (www.preprints.org) | NOT PEER-REVIEWED | Posted: 13 July 2018 doi:10.20944/preprints201807.0226.v1

previously described nanocages can be achieved through essentially the same galvanic replacement, but they are specific nanostructures that are only obtained from specific types of Ag nanotemplates. Theoretically, a 3D template with a height dimension along with a basal plane forms a cage-like structure including hollow nanoshell derivatives. However, templates with relatively short height that do not tolerate structural transformation during galvanic replacement form edge-replaced and basal-plane-dissolved nanostructures, which are often referred to as ring-shaped nanostructures. The most commonly used templates are round-shaped Ag nanodisks [172-175] and Ag nanoplates [176-179] or nanoprisms [180-185], which form nanorings and nanoframes, respectively. Although there are various types according to shape, they all have in common excellent NIR photothermal conversion efficiencies, which is advantageous for *in vivo* cancer treatment, and are easy to load with relatively bulky cargoes both inside and outside due to their surface opened skeletal nanostructures. In addition, unlike hollow nanoshells, which are formed from the dissolution of relatively large amounts of template Ag, unintended cytotoxicity derived from dissolved Ag and reactive-oxygen-species generation are minimized. Therefore, nanoframes are more suitable for *in vivo* biomedical applications owing to their higher biocompatibility. However, research into the general application of nanoframes is still in its initial stages because precise reaction conditions are required for their synthesis. Currently, nanoframes themselves are used as templates to provide desired functionality and characteristics by secondary growth or transformation.

2.2. Extended shapes by modified galvanic replacement

Beyond the drawbacks in nanostructure formation by conventional galvanic replacement, such as nanostructural collapse and aggregation under stoichiometric overdose, template surface poisoning by precipitation of insoluble adducts, and the limited number of element pairs suitable for spontaneous redox reaction, numerous efforts are underway to address the current limits. The introduction of new nanostructures suitable for cancer treatment through galvanic replacement has been achieved through these various attempts, and several chemical principles and possibilities are discussed herein.

2.2.1. Porous nanostructures

Porous nanoparticles of metal oxide nanomaterials such as mesoporous silica (SiO_2) [186-193], and mesoporous titania (TiO_2) [194-199] have been extensively studied owing to their facile template assisted

 doi:10.20944/preprints201807.0226.v1

formation. In the case of noble metal nanoparticles, no methods for the controlled synthesis of porous nanostructures have been established owing to the need for reducing-agent-mediated synthetic strategies and the importance of crystallinity. Nonetheless, because of the extremely high surface-to-volume ratios and structural advantages of porous nanostructures, the development of new synthetic methods for noble metals has been a subject of increasing interest [200-211]. The synthesis of porous Au nanoparticles using Ag nanospheres was first achieved through an extended synthetic strategy called inhibitory galvanic replacement. In inhibitory galvanic replacement, the formation of the AgCl adduct, which is a byproduct of conventional galvanic replacement, is intentionally maximized through a low-temperature reaction in order to partially block the replacement reaction [212]. Then, the embedded Au structures are revealed through the addition of excess hydrogen peroxide, which is an effective etchant for Ag and AgCl. As a result, spherically clustered porous Au nanostructures are obtained and, because of their partially connected clustered structures, an entire LSPR band in the visible-NIR range that is suitable for photothermal cancer treatment appears. In porous Au nanoparticles synthesized by inhibitory galvanic replacement, nitrogen adsorption analysis reveals a pore diameter of ≈3.4 nm, which implies that oligonucleotides can be effectively loaded and delivered. Porous Au nanoparticles exhibit significantly enhanced gene delivery efficiency compared that of hollow Au nanoshells, which have been used in conventional studies, in the loading and delivery of the small anticancer compound doxorubicin and fluorescently labelled oligonucleotides. This represents the conversion of AgCl adduct precipitation, which is regarded as a drawback of conventional galvanic replacement, to a positive phenomenon, and it is expected that various further applications of the advanced nanostructures formed will be possible.

Structural transformation can vary widely depending on the type of template nanostructure employed and can lead to dramatic differences for flat-surface containing nanostructures such as nanocubes and nanoplates with a high surface-to-volume ratio that enables rapid galvanic replacement. An example of nanoplate-based porous nanostructure formation and cancer treatment is provided by a new synthetic method that is an improvement of conventional galvanic replacement [213]. Conventionally, galvanic replacement of nanoplates is known to result in nanoframes or nanorings, in which all internal spaces are removed, rather than hollow nanoshells, and excessive cation addition causes fragmentation, as in other cases. The disadvantage of spatial structures can be overcome by regulating the competition between replacement and regrowth rate through the addition of various reducing agents, such as L-ascorbic acid, during the galvanic replacement process. The galvanic replacement takes precedence over the initial high concentration of replacing cations, forming a

Preprints (www.preprints.org) | NOT PEER-REVIEWED | Posted: 13 July 2018 doi:10.20944/preprints201807.0226.v1

nanoframe-shaped secondary template, and the depletion of the replacing cation through galvanic replacement shifts the reaction equilibrium to regrowth, resulting in surface growth from the secondary template. This surface growth is attributed to the fact that the reducing agent in the solution forms a partially reduced replacing cation species, which can lead to nondestructive structural transformation, even in excess conditions. This reducing-agent-assisted galvanic replacement forms porous Au nanoplate structures, which exhibit high absorption in the NIR region. Through the optical properties of porous Au nanoplates and the high affinity between thiolated cargoes and the Au surface, thiolated-oligonucleotide loading/releasing and photothermal cancer treatments based on NIR laser irradiation have allowed combinational gene-thermo cancer therapy to be accomplished with excellent efficiency.

As discussed above, additional reaction modulation factors such as temperature, post-synthetic etching, and reductive additives have allowed the formation of porous Au nanostructures that could not be synthesized with conventional galvanic replacements. Porous Au nanostructures have a higher surface-to-volume ratio because of surface roughness compared to similar structures having smooth surfaces, leading to enhancement of the overall absorbance characteristics in the UV-Vis-NIR region by their networked substructures. As a result, it is possible to induce the photothermal conversion effect by light irradiation of various wavelengths, and it is advantageous to selectively apply an NIR wavelength suitable for photothermal cancer treatment. Moreover, based on their structural specificity, they are more appropriate for gene delivery than Au nanorods or nanocages, which have been the most common candidates for cancer treatment. The only disadvantage of these porous nanostructures is the difficulty in quantifying the number of nanoparticles in solution. Replacement and regrowth have been competitively accomplished to form monodisperse but irregular nanostructures, meaning that accurate quantification techniques have not been developed, unlike for well-ordered nanospheres, nanorods, and nanocubes. It has been assumed that the Ag template used is completely transformed into the desired nanostructure without disappearing during galvanic replacement, and its concentration has been quantified. Further studies on this will provide major contributions to biomedical applications that have large concentration effects. Despite these present disadvantages, porous nanostructures have received a great deal of attention recently in many research fields owing to their extremely high surface-to-volume ratios and unique physicochemical properties, and the same is true for cancer treatment.

2.2.2. Anisotropic nanostructures

 doi:10.20944/preprints201807.0226.v1

Anisotropic metal nanoparticles are considered to be of interest in variety of applications because of their various physicochemical properties resulting from their structural specificity, which is also a key feature in cancer treatment. The most common examples are nanostars, sea-urchin like nanoparticles, and nanoworms, and various functionalities such as photothermal therapeutics, surface enhanced Raman scattering (SERS), and magnetic resonance (MR) imaging are possible depending on the constituent metal elements [214-221]. In general, the synthesis of anisotropic nanoparticles is controlled by regulatable molecules including solvents, surfactants, peptides, and polymers through diffusion rate and growth kinetics modulation. Here, we introduce the synthesis and cancer-treatment applications of anisotropic nanoparticles formed by galvanic replacement.

Because galvanic replacement is a reaction based on spontaneous element exchange and growth in heterogeneous systems, the diffusion and approach of metal cations, which can affect these factors, is regarded as a major concern. In this regard, a rough mechanism has been revealed through various structure formation tendencies depending on pH, temperature, and additives. However, because of the contribution of numerous critical factors, it is difficult to develop a precisely designed synthetic method. According to Zhang et al., the interaction between a Cu template and the replacing Pt can be confirmed by the fact that the size and number of hollow voids, which are the most important features of nanostructures formed through galvanic replacement, can be varied depending on pH and the presence of the surface-stabilizing polymer PVP [222]. These adjustments result in the formation of nanoboxes, heterodimers, multimers, and popcorn-shaped hollow voids. These are interpreted as a result of diffusion rate control, which affects the redox reaction between the template and the replacing cation. Although the nanoparticles formed are not utilized in practical biomedical applications, approaches based on the diffusion rate as a core mechanism from the viewpoint of functionally enhanced nanoparticle formation encompass several possibilities. Diffusion contributes to the number of collisions between metal elements for replacement, but it also has an important effect on the directionality of the structure being formed and extended. This is related to the Kirkendall effect at the interface between the formed metal and the alloy. Depending on the geometry of the voids formed and the contact type, the formation of porous or rough surfaces or the formation of conventional nanocages are determined. Furthermore, it is possible to confirm that a dendritic nanostructure is formed through position-limited diffusion control where the replacing cation contacts for replacement. However, if the focus is on the physicochemical and optical properties to be derived, these kinds of structures may be more suitable for biomedical applications than conventional hollow nanostructures.

Another interesting approach to the manufacture of anisotropic nanoparticles for cancer treatment is

Preprints (www.preprints.org) | NOT PEER-REVIEWED | Posted: 13 July 2018 doi:10.20944/preprints201807.0226.v1

partially polymer-coated Au nanoworms [223]. The nanostructures formed by the excessive galvanic replacement of a Ag nanoparticle template coated with the biocompatible polymer dextran are formed in a way by which the whole connection structure is maintained but the spherical structure is destroyed. This non-conservative replacement forms a complex nanostructure that is partially covered with a dextran shell with the remainder being an exposed bare Au surface. The independent structures of the bare Au surface and partial dextran shell can be applied to chemotherapy separately. Chemical affinity-based loading of a thiolated-cargo on the exposed Au surface and chemical bonding-based loading exploiting the abundant hydroxyl functionality of dextran allows the simultaneous loading of two different therapeutic cargos onto the nanostructure. In addition, NIR plasmonic photothermal conversion by the anisotropic nanostructures results in excellent efficacy in combinational cancer treatment using hyperthermic therapy.

As the series of examples above shows, studies on the formation of anisotropic Au nanostructures and sophisticated Au nanostructures using modified galvanic replacement have been actively conducted. Based on the physicochemical properties derived from the structures, various application techniques have been devised that are significantly different from those available with conventional hollow nanoshell or nanocage structures. The synthetic advantage of being able to form high-order nanostructures without the use of toxic surfactants facilitates their application in numerous application fields. Many cancer-treatment studies have been conducted based on their excellent photothermal conversion and therapeutic cargo payload capabilities.

3. Composition control by galvanic replacement

Research on the synthesis of nanoparticles of various shapes and compositions has attracted much attention because composition contributes to the physicochemical properties of the particles as much as morphology. However, the synthesis of nanoparticles with the same morphology and size but with different constituent elements cannot be achieved easily because of various factors such as the crystal structure, atomic size, and electron configuration of each element. Galvanic replacement has been widely applied to the formation of such nanoparticles owing to its template-based elemental replacement reaction manner.

3.1. Platinum-group elements

 doi:10.20944/preprints201807.0226.v1

In general, Ru, Os, Rh, Ir, Pd, and Pt are referred as platinum-group elements. Ag is most commonly used as a template for galvanic replacement because it forms various structures easily and is cheap. Only Au, Pd, and Pt can be applied under ambient conditions for voluntary redox replacement of Ag. However, in order to provide more scope for structural formation and the applications of galvanic replacement, there is a need to expand these element pairs, and the most important candidate is the platinum group source used in various fields, including catalysis. Because platinum-group nanoparticles are known to exhibit UV-restricted LSPR spectra and are relatively expensive and toxic compared to Au-based nanoparticles, their application to biomedical applications is relatively restricted. However, some recent studies have reported interesting properties in the case of porous Pt and Pd nanoparticles, such as efficient light absorption in the visible and NIR wavelength region. This suggests that new possibilities for platinum-group elements may be developed if systematic and quantitative research is supported. Recently, quantitative comparisons of these possibilities have been made through the formation of porous Au, Pt, and Pd nanoplates through reducing-agent-assisted excessive galvanic replacement [224]. For example, Kang et al. compared the cytotoxicities, gene loading efficiencies, photothermal conversion efficiencies, and combinational cancer treatment applicabilities of porous nanoplates composed of Au, Pt, and Pd with similar sizes and morphologies prepared using the same Ag nanotemplate. Interestingly, Pd was superior to Au, which was previously considered to be superior in all ways. Even in terms of price, Pd is cheaper than Au, which means that in future cancer treatment research based on nanoparticles, more attention should be paid to new element-based approaches beyond established norms.

Another example of the galvanic replacement of Ag templates by platinum-group elements is the specific response of Rh. Since Rh^{3+} exhibits a lower standard reduction potential than that of Ag, conventional galvanic replacement cannot occur under ambient conditions. However, in two recent cases, Cu template mediated galvanic replacement [225-228] and a spontaneous response was derived using Nernst-equation-based reasoning by controlling the temperature and concentration so that the whole cell voltage was positive [229]. This approach allowed the formation of hollow Rh nanoshells, Rh nanoframes, and porous Rh nanoplates, respectively. Furthermore, the biomedical potential for Rh nanoparticles, which is widely used in conventional hydrogen generation catalyst applications, has been demonstrated. It is important that there are no biological study results regarding the cytotoxicity of Rh owing to the current limitations of its application. According to *in vitro* and *in vivo* analyses, Rh nanoparticles formed through inverse galvanic replacement showed biocompatibility and photothermal conversion efficiency comparable to those of Au [229]. In actual cancer treatment applications,

 doi:10.20944/preprints201807.0226.v1

photothermal therapy was performed after conjugation with TAT, which is a cell-penetrating peptide, allowing introduction into cells and cancer tissues. Although there has been no application to actual cancer treatment, galvanic replacement with other platinum-group elements has received some attention recently. However, only galvanic replacement of Ru, Os, and Ir using a Cu template because of their low reduction potentials is known, and physicochemical characterization and potential verification of these are currently insufficient. As in the case of Rh, the application to biomedical applications, including cancer treatment, of platinum-group elements has tremendous possibilities [230-235]. Consequently, a suitable synthetic platform and systematic analysis are urgently required.

3.2. Other transition metal elements

Unlike general galvanic replacement, which requires a metal templates such as Ag, Cu, and Ni, a new approach using metal oxides as a template was first reported in 2013 by Hyeon et al [236]. In this pioneering work, a hollow bimetallic oxide nanoparticle was produced by post-synthetic transformation using the oxidation-reduction reaction between oxidized water, taking into account that the transition metal may have various oxidation forms. Although not directly applicable to biomedical applications, Mn and Fe used in the study have potential as MR imaging contrast agents and magnetic properties that allow site-specific concentration *in vivo* [237-242]. Based on the myriad of transition-metal nanoparticles present in the form of metal oxides and the ability to mass-synthesize them, this approach is an example of extended galvanic replacement and can be viewed as a new and feasible approach for the future.

4. Conclusion

Synthesis of various interesting nanostructures through galvanic replacement and cancer treatment based on drug delivery and plasmonic photothermal therapy have been introduced. The development of methods for structurally and compositionally regulated nanoparticle synthesis is regarded as a key element for future nanotherapeutics and improving the safety and efficiency of nanoparticle mediated cancer treatments. To this end, galvanic replacement, which is used to synthesize complex structures via an environmentally friendly and convenient procedure, has reached beyond what was thought possible through continuous improvement. Many of the metal elements that form nanoparticles are not being exploited in biomedical applications because of factors

 doi:10.20944/preprints201807.0226.v1

such as high-price, toxicity, and instability. However, by introducing the possibility of overcoming these general disadvantages through the regulation of structure and composition, we believe that continuous interest and research will bring new vitality to the field of biological research including cancer treatment.

AUTHOR INFORMATION

Corresponding Author

*Hongje Jang

Phone: +82-2-940-8320. E-mail: hjang@kw.ac.kr

AUTHOR CONTRIBUTIONS

‡Woojun Shin and Kyungtae Kang contributed equally.

ACKNOWLEDGEMENT

This work was supported by National Research Foundation of Korea (NRF) funded by Korean government (Grant Nos. 2016R1C1B1008090).

REFERENCES

1. National Cancer Institute. *Defining Cancer.* Retrived 10 June **2014**.
2. World Health Organization. *World Cancer Report.* **2014**, Chapter 1.1.
3. Bomford, C. K.; Kunkler, I. H. *Walter and Miller's Textbook of Radiation Therapy, 6th* Ed, p311.
4. Vickers, A. Alternative Cancer Cures: "Unproven" or "Disproven"? *CA. Cancer J. Clin.* **2004**, *54* (2), 110–118.
5. Cassileth, B. R.; Deng, G. Complementary and Alternative Therapies for Cancer. *Oncologist* **2004**, *9*, 80-89.

6. Barberis, I.; Martini, M.; Iavarone, F.; Orsi, A. Available Influenza Vaccines: Immunization Strategies, History and New Tools for Fighting the Disease. *J. Prev. Med. Hyg.* **2016**, *57* (1), E41–E46.
7. Waldmann, T. A. Immunotherapy: Past, Present and Future. *Nat. Med.* **2003**, *9* (3), 269–277.
8. Oak, C. H.; Wilson, D.; Lee, H. J.; Lim, H.-J.; Park, E.-K. Potential Molecular Approaches for the Early Diagnosis of Lung Cancer (Review). *Mol. Med. Rep.* **2012**, *6* (5), 931–936.
9. Zhang, Q.; Chen, S.; Zeng, L.; Chen, Y.; Lian, G.; Qian, C.; Li, J.; Xie, R.; Huang, K. H. New Developments in the Early Diagnosis of Pancreatic Cancer. *Expert Rev Gastroenterol Hepatol* **2016**, *0* (0), 1–8.
10. Hamilton, W.; Walter, F. M.; Rubin, G.; Neal, R. D. Improving Early Diagnosis of Symptomatic Cancer. *Nat. Rev. Clin. Oncol.* **2016**, *13* (12), 740–749.
11. Chari, S. T.; Kelly, K.; Hollingsworth, M. a; Sarah, P.; Ahlquist, D. a; Andersen, D. K.; Batra, S. K.; Brentnall, T. a; Canto, M.; Deborah, F.; et al. Early Detection of Sporadic Pancreatic Cancer. *Pancreas* **2015**, *44* (5), 693–712.
12. Rubin, G.; Berendsen, A.; Crawford, S. M.; Dommett, R.; Earle, C.; Emery, J.; Fahey, T.; Grassi, L.; Grunfeld, E.; Gupta, S.; et al. The Expanding Role of Primary Care in Cancer Control. *Lancet Oncol.* **2015**, *16* (12), 1231–1272.
13. Benjamin, D. J. The Efficacy of Surgical Treatment of Cancer - 20 Years Later. *Med. Hypotheses* **2014**, *82* (4), 412–420.
14. Gustavsson, B.; Carlsson, G.; MacHover, D.; Petrelli, N.; Roth, A.; Schmoll, H. J.; Tveit, K. M.; Gibson, F. A Review of the Evolution of Systemic Chemotherapy in the Management of Colorectal Cancer. *Clin. Colorectal Cancer* **2015**, *14* (1), 1–10.
15. Chabner, B. A.; Roberts, T. G. Timeline: Chemotherapy and the War on Cancer. *Nat. Rev. Cancer* **2005**, *5* (1), 65–72.
16. Huang, C.-Y.; Ju, D.-T.; Chang, C.-F.; Muralidhar Reddy, P.; Velmurugan, B. K. A Review on the Effects of Current Chemotherapy Drugs and Natural Agents in Treating Non–small Cell Lung Cancer. *BioMedicine* **2017**, *7* (4), 23.

17. Del Paggio, J. C.; Sullivan, R.; Schrag, D.; Hopman, W. M.; Azariah, B.; Pramesh, C. S.; Tannock, I. F.; Booth, C. M. Delivery of Meaningful Cancer Care: A Retrospective Cohort Study Assessing Cost and Benefit with the ASCO and ESMO Frameworks. *Lancet Oncol.* **2017**, *18* (7), 887–894.
18. Tran, S.; DeGiovanni, P.-J.; Piel, B.; Rai, P. Cancer Nanomedicine: A Review of Recent Success in Drug Delivery. *Clin. Transl. Med.* **2017**, *6* (1), 44.
19. Colone, M.; Kaliappan, S.; Calcabrini, A.; Tortora, M.; Stringaro, A. Drug Delivery System and Breast Cancer Cells. **2016**, *020013* (2016), 020013.
20. Achantal, A. S.; Kowalski, J. G.; Moses, M. A.; Brem, H.; Langer, R.; Celia, C.; Trapasso, E.; Locatelli, M.; Navarra, M.; Ventura, C. A.; et al. Antitumor Activity of (Trans)Dermally Delivered Aromatic Tetra-Amidines. *Drug Dev. Ind. Pharmacy,* **2013**, *4* (5), 119–155.
21. Mendes, R.; Pedrosa, P.; Lima, J. C.; Fernandes, A. R.; Baptista, P. V. Photothermal Enhancement of Chemotherapy in Breast Cancer by Visible Irradiation of Gold Nanoparticles. *Sci. Rep.* **2017**, *7* (1), 1–9.
22. Zou, L.; Wang, H.; He, B.; Zeng, L.; Tan, T.; Cao, H.; He, X.; Zhang, Z.; Guo, S.; Li, Y. Current Approaches of Photothermal Therapy in Treating Cancer Metastasis with Nanotherapeutics. *Theranostics* **2016**, *6* (6), 762–772.
23. Chen, F.; Cai, W. Nanomedicine for Targeted Photothermal Cancer Therapy: Where Are We Now? *Nanomedicine* **2015**, *10* (1), 1–3.
24. Kolovskaya, O. S.; Zamay, T. N.; Belyanina, I. V.; Karlova, E.; Garanzha, I.; Aleksandrovsky, A. S.; Kirichenko, A.; Dubynina, A. V.; Sokolov, A. E.; Zamay, G. S.; et al. Aptamer-Targeted Plasmonic Photothermal Therapy of Cancer. *Mol. Ther. - Nucleic Acids* **2017**, *9* (December), 12–21.
25. Felsher, D. W. Cancer Revoked: Oncogenes as Therapeutic Targets. *Nat. Rev. Cancer* **2003**, *3* (5), 375–380.
26. Agostinis, P.; Berg, K.; Cengel, K. .; Foster, T. .; Girotti, A. .; Gollnick, S. .; Hahn, S. .; Hamblin, M. .; Juzeniene, A.; Kessel, D.; et al. Photodynamic Terapy of Cancer: An Update. *CA Cancer J Clin.* **2011**, *61* (4), 250–281.
27. Brown, S. B.; Brown, E. a; Walker, I. The Present and Future Role of Photodynamic Therapy in Cancer Treatment. *Lancet Oncol.* **2004**, *5* (8), 497–508.
28. Azzouzi, A. R.; Vincendeau, S.; Barret, E.; Cicco, A.; Kleinclauss, F.; van der Poel, H. G.; Stief, C. G.;

Rassweiler, J.; Salomon, G.; Solsona, E.; et al. Padeliporfin Vascular-Targeted Photodynamic Therapy versus Active Surveillance in Men with Low-Risk Prostate Cancer (CLIN1001 PCM301): An Open-Label, Phase 3, Randomised Controlled Trial. *Lancet Oncol.* **2017**, *18* (2), 181–191.

29. Talapin, D. V.; Shevchenko, E. V. Introduction: Nanoparticle Chemistry. *Chem. Rev.* **2016**, *116* (18), 10343–10345.
30. Khan, I.; Saeed, K.; Khan, I. Nanoparticles: Properties, Applications and Toxicities. *Arab. J. Chem.* **2017**.
31. Grigore, M. E.; Biscu, E. R.; Holban, A. M.; Gestal, M. C.; Grumezescu, A. M. Methods of Synthesis, Properties and Biomedical Applications of CuO Nanoparticles. *Pharmaceuticals* **2016**, *9* (4), 1–14.
32. Angioletti-Uberti, S. Theory, Simulations and the Design of Functionalized Nanoparticles for Biomedical Applications: A Soft Matter Perspective. *npj Comput. Mater.* **2017**, *3* (1), 1–15.
33. McNamara, K.; Tofail, S. A. M. Nanoparticles in Biomedical Applications. *Adv. Phys. X* **2017**, *2* (1), 54–88.
34. Kumari, P.; Ghosh, B.; Biswas, S. Nanocarriers for Cancer-Targeted Drug Delivery. *J. Drug Target.* **2016**, *24* (3), 179–191.
35. Li, Z.; Tan, S.; Li, S.; Shen, Q.; Wang, K. Cancer Drug Delivery in the Nano Era: An Overview and Perspectives (Review). *Oncol. Rep.* **2017**, *38* (2), 611–624.
36. Jain, P. K.; Huang, X.; El-Sayed, I. H.; El-Sayed, M. A. Review of Some Interesting Surface Plasmon Resonance-Enhanced Properties of Noble Metal Nanoparticles and Their Applications to Biosystems. *Plasmonics* **2007**, *2* (3), 107–118.
37. Iatì, V. A. and R. P. and M. F. and O. M. M. and M. A. Surface Plasmon Resonance in Gold Nanoparticles: A Review. *J. Phys. Condens. Matter* **2017**, *29* (20), 203002.
38. Takagahara, T.; Takeda, K. Theory of the Quantum Confinement Effect on Excitons in Quantum Dots of Indirect-Gap Materials. *Phys. Rev. B* **1992**, *46* (23), 15578–15581.
39. Melgaard, M. Confinement Effects on Scattering for a Nanoparticle. *Acta Phys. Pol. B* **2007**, *38* (1), 197–214.
40. Zhou, H. S.; Honma, I.; Komiyama, H.; Haus, J. W. Controlled Synthesis and Quantum-Size Effect in Gold-Coated Nanoparticles. *Phys. Rev. B* **1994**, *50* (16), 12052–12056.

41. Chen, Q.; Qi, H.; Ren, Y. T.; Sun, J. P.; Ruan, L. M. Optical Properties of Truncated Au Nanocages with Different Size and Shape. *AIP Adv.* **2017**, *7* (6).

42. Lee, H.; Habas, S. E.; Kweskin, S.; Butcher, D.; Somorjai, G. A.; Yang, P. Morphological Control of Catalytically Active Platinum Nanocrystals. *Angew. Chemie - Int. Ed.* **2006**, *45* (46), 7824–7828.

43. Miyazaki, A.; Balint, I.; Nakano, Y. Morphology Control of Platinum Nanoparticles and Their Catalytic Properties. **2003**, 69–80.

44. Sau, T. K.; Rogach, A. L. Nonspherical Noble Metal Nanoparticles: Colloid-Chemical Synthesis and Morphology Control. *Adv. Mater.* **2010**, *22* (16), 1781–1804.

45. Huang, X.; Neretina, S.; El-Sayed, M. A. Gold Nanorods: From Synthesis and Properties to Biological and Biomedical Applications. *Adv. Mater.* **2009**, *21* (48), 4880–4910.

46. Yang, S.; Luo, X. Mesoporous Nano/Micro Noble Metal Particles: Synthesis and Applications. *Nanoscale* **2014**, *6* (9), 4438–4457.

47. Lee, K. S.; El-Sayed, M. A. Gold and Silver Nanoparticles in Sensing and Imaging: Sensitivity of Plasmon Response to Size, Shape, and Metal Composition. *J. Phys. Chem. B* **2006**, *110* (39), 19220–19225.

48. Khan, I.; Saeed, K.; Khan, I. Nanoparticles: Properties, Applications and Toxicities. *Arab. J. Chem.* **2017**.

49. Tajammul Hussain, S.; Iqbal, M.; Mazhar, M. Size Control Synthesis of Starch Capped-Gold Nanoparticles. *J. Nanoparticle Res.* **2009**, *11* (6), 1383–1391.

50. Cuenya, B. R. Synthesis and Catalytic Properties of Metal Nanoparticles: Size, Shape, Support, Composition, and Oxidation State Effects. *Thin Solid Films* **2010**, *518* (12), 3127–3150.

51. Rehn, S. M.; Ringe, E. Controllably Hollow AgAu Nanoparticles via Nonaqueous, Reduction Agent-Assisted Galvanic Replacement. *Part. Part. Syst. Charact.* **2018**, *1700381*, 1700381.

52. Chen, J.; Wiley, B.; McLellan, J.; Xiong, Y.; Li, Z. Y.; Xia, Y. Optical Properties of Pd-Ag and Pt-Ag Nanoboxes Synthesized via Galvanic Replacement Reactions. *Nano Lett.* **2005**, *5* (10), 2058–2062.

53. Kranich, A.; Naumann, H.; Molina-heredia, F. P.; Moore, J.; Lee, T. R.; Lecomte, S.; De, M. A.; Hildebrandt, P.; Murgida, D. H.; Chem, P.; et al. Quo Vadis Surface-Enhanced Raman Scattering? *Phys. Chem. Chem. Phys.* **2009**, *11* (34), 7348.

54. Jain, P. K.; Lee, K. S.; El-Sayed, I. H.; El-Sayed, M. A. Calculated Absorption and Scattering Properties of Gold Nanoparticles of Different Size, Shape, and Composition: Applications in Biological Imaging and Biomedicine. *J. Phys. Chem. B* **2006**, *110* (14), 7238–7248.

55. Gurunathan, S.; Han, J. W.; Park, J. H.; Kim, J. H. A Green Chemistry Approach for Synthesizing Biocompatible Gold Nanoparticles. *Nanoscale Res. Lett.* **2014**, *9* (1), 1–11.

56. Yah, Clarence S. The Toxicity of Gold Nanoparticles in Relation to Their Physicochemical Properties. *Biomed. Res.* **2013**, *24* (3), 400–413.

57. Sun, I. C.; Na, J. H.; Jeong, S. Y.; Kim, D. E.; Kwon, I. C.; Choi, K.; Ahn, C. H.; Kim, K. Biocompatible Glycol Chitosan-Coated Gold Nanoparticles for Tumor-Targeting CT Imaging. *Pharm. Res.* **2014**, *31* (6), 1418–1425.

58. Santos-Martinez, M. J.; Rahme, K.; Corbalan, J. J.; Faulkner, C.; Holmes, J. D.; Tajber, L.; Medina, C.; Radomski, M. W. Pegylation Increases Platelet Biocompatibility of Gold Nanoparticles. *J. Biomed. Nanotechnol.* **2014**, *10* (6), 1004–1015.

59. Jain, S.; Hirst, D. G.; O'Sullivan, J. M. Gold Nanoparticles as Novel Agents for Cancer Therapy. *Br. J. Radiol.* **2012**, *85* (1010), 101–113.

60. Dykman, L. A.; Khlebtsov, N. G. Uptake of Engineered Gold Nanoparticles into Mammalian Cells. *Chem. Rev.* **2014**, *114* (2), 1258–1288.

61. Muddineti, O. S.; Ghosh, B.; Biswas, S. Current Trends in Using Polymer Coated Gold Nanoparticles for Cancer Therapy. *Int. J. Pharm.* **2015**, *484* (1–2), 252–267.

62. Grant, S. A.; Spradling, C. S.; Grant, D. N.; Fox, D. B.; Jimenez, L.; Grant, D. A.; Rone, R. J. Assessment of the Biocompatibility and Stability of a Gold Nanoparticle Collagen Bioscaffold. *J. Biomed. Mater. Res. - Part A* **2014**, *102* (2), 332–339.

63. Shah, M.; Badwaik, V. D.; Dakshinamurthy, R. Biological Applications of Gold Nanoparticles. *J. Nanosci. Nanotechnol.* **2014**, *14* (1), 344–362.

64. Jang, H.; Kim, Y. -K.; Ryoo, S. -R.; Kim, M. -H.; Min, D. -H. Facile Synthesis of Robust and Biocompatible Gold Nanoparticles. *Chem. Commun.* **2010**, *46*, 583-585.

65. Pooja, D.; Panyaram, S.; Kulhari, H.; Reddy, B.; Rachamalla, S. S.; Sistla, R. Natural Polysaccharide Functionalized Gold Nanoparticles as Biocompatible Drug Delivery Carrier. *Int. J. Biol. Macromol.* **2015**, *80*, 48–56.

66. Daraee, H.; Eatemadi, A.; Abbasi, E.; Aval, S. F.; Kouhi, M.; Akbarzadeh, A. Application of Gold Nanoparticles in Biomedical and Drug Delivery. *Artif. Cells, Nanomedicine Biotechnol.* **2016**, *44* (1), 410–422.

67. Mieszawska, A. J.; Mulder, W. J. M.; Fayad, Z. A.; Cormode, D. P. Multifunctional Gold Nanoparticles for Diagnosis and Therapy of Disease. *Mol. Pharm.* **2013**, *10* (3), 831–847.

68. Sun, Y.; Xia, Y. Alloying and Dealloying Processes Involved in the Preparation of Metal Nanoshells through a Galvanic Replacement Reaction. *Nano Lett.* **2003**, *3* (11), 1569–1572.

69. Yang, X.; Roling, L. T.; Vara, M.; Elnabawy, A. O.; Zhao, M.; Hood, Z. D.; Bao, S.; Mavrikakis, M.; Xia, Y. Synthesis and Characterization of Pt-Ag Alloy Nanocages with Enhanced Activity and Durability toward Oxygen Reduction. *Nano Lett.* **2016**, *16* (10), 6644–6649.

70. Yang, Y.; Zhang, Q.; Fu, Z. W.; Qin, D. Transformation of Ag Nanocubes into Ag-Au Hollow Nanostructures with Enriched Ag Contents to Improve SERS Activity and Chemical Stability. *ACS Appl. Mater. Interfaces* **2014**, *6* (5), 3750–3757.

71. Gong, J.; Zhou, F.; Li, Z.; Tang, Z. Synthesis of Au@Ag Core-Shell Nanocubes Containing Varying Shaped Cores and Their Localized Surface Plasmon Resonances. *Langmuir* **2012**, *28* (24), 8959–8964.

72. Jenkins, S. V.; Gohman, T. D.; Miller, E. K.; Chen, J. Synthesis of Hollow Gold-Silver Alloyed Nanoparticles: A “Galvanic Replacement” Experiment for Chemistry and Engineering Students. *J. Chem. Educ.* **2015**, *92* (6), 1056–1060.

73. Jiang, Y.; Lu, Y.; Han, D.; Zhang, Q.; Niu, L. Hollow Ag@Pd Core-Shell Nanotubes as Highly Active Catalysts for the Electro-Oxidation of Formic Acid. *Nanotechnology* **2012**, *23* (10).

74. Liu, D.; Xie, M.; Wang, C.; Liao, L.; Qiu, L.; Ma, J.; Huang, H.; Long, R.; Jiang, J.; Xiong, Y. Pd-Ag Alloy Hollow Nanostructures with Interatomic Charge Polarization for Enhanced Electrocatalytic Formic Acid Oxidation. *Nano Res.* **2016**, *9* (6), 1590–1599.

75. Xu, L.; Luo, Z.; Fan, Z.; Zhang, X.; Tan, C.; Li, H.; Zhang, H.; Xue, C. Triangular Ag-Pd Alloy Nanoprisms: Rational Synthesis with High-Efficiency for Electrocatalytic Oxygen Reduction. *Nanoscale* **2014**, *6* (20), 11738–11743.

76. Wu, H.; Wang, P.; He, H.; Jin, Y. Controlled Synthesis of Porous Ag/Au Bimetallic Hollow Nanoshells with Tunable Plasmonic and Catalytic Properties. *Nano Res.* **2012**, *5* (2), 135–144.

77. Karvianto; Chow, G. M. Size-Dependent Transformation from Ag Templates to Au-Ag Nanoshells via Galvanic Replacement Reaction in Organic Medium. *J. Nanoparticle Res.* **2012**, *14* (10).

78. Jing, H.; Wang, H. Structural Evolution of Ag-Pd Bimetallic Nanoparticles through Controlled Galvanic Replacement: Effects of Mild Reducing Agents. *Chem. Mater.* **2015**, *27* (6), 2172–2180.

79. Petri, M. V.; Ando, R. A.; Camargo, P. H. C. Tailoring the Structure, Composition, Optical Properties and Catalytic Activity of Ag-Au Nanoparticles by the Galvanic Replacement Reaction. *Chem. Phys. Lett.* **2012**, *531*, 188–192.

80. Yang, Y.; Liu, J.; Fu, Z. W.; Qin, D. Galvanic Replacement-Free Deposition of Au on Ag for Core-Shell Nanocubes with Enhanced Chemical Stability and SERS Activity. *J. Am. Chem. Soc.* **2014**, *136* (23), 8153–8156.

81. Polavarapu, L.; Liz-Marzán, L. M. Growth and Galvanic Replacement of Silver Nanocubes in Organic Media. *Nanoscale* **2013**, *5* (10), 4355–4361.

82. Bin, D.; Yang, B.; Zhang, K.; Wang, C.; Wang, J.; Zhong, J.; Feng, Y.; Guo, J.; Du, Y. Design of PdAg Hollow Nanoflowers through Galvanic Replacement and Their Application for Ethanol Electrooxidation. *Chem. - A Eur. J.* **2016**, *22* (46), 16642–16647.

83. Polavarapu, L.; Zanaga, D.; Altantzis, T.; Rodal-Cedeira, S.; Pastoriza-Santos, I.; Pérez-Juste, J.; Bals, S.; Liz-Marzán, L. M. Galvanic Replacement Coupled to Seeded Growth as a Route for Shape-Controlled Synthesis of Plasmonic Nanorattles. *J. Am. Chem. Soc.* **2016**, *138* (36), 11453–11456.

84. Tsuji, M.; Kidera, T.; Yajima, A.; Hamasaki, M.; Hattori, M.; Tsuji, T.; Kawazumi, H. Synthesis of Ag-Au and Ag-Pd Alloy Triangular Hollow Nanoframes by Galvanic Replacement Reactions without and with Post-Treatment Using NaCl in an Aqueous Solution. *CrystEngComm* **2014**, *16* (13), 2684–2691.

85. Da Silva, A. G. M.; De Souza, M. L.; Rodrigues, T. S.; Alves, R. S.; Temperini, M. L. A.; Camargo, P. H. C. Rapid Synthesis of Hollow Ag-Au Nanodendrites in 15 Seconds by Combining Galvanic Replacement and Precursor Reduction Reactions. *Chem. - A Eur. J.* **2014**, *20* (46), 15040–15046.

86. Li, Q.; Xu, P.; Zhang, B.; Wu, G.; Zhao, H.; Fu, E.; Wang, H. L. Self-Supported Pt Nanoclusters via Galvanic Replacement from Cu2O Nanocubes as Efficient Electrocatalysts. *Nanoscale* **2013**, *5* (16), 7397–7402.

87. Xu, C.; Liu, Y.; Wang, J.; Geng, H.; Qiu, H. Fabrication of Nanoporous Cu-Pt(Pd) Core/Shell Structure by Galvanic Replacement and Its Application in Electrocatalysis. *ACS Appl. Mater. Interfaces* **2011**, *3* (12), 4626–4632.

88. Yao, W.; Li, F.-L.; Li, H.-X.; Lang, J.-P. Fabrication of Hollow Cu_2O@CuO-Supported Au–Pd Alloy Nanoparticles with High Catalytic Activity through the Galvanic Replacement Reaction. *J. Mater. Chem. A* **2015**, *3* (8), 4578–4585.

89. Wang, S. B.; Zhu, W.; Ke, J.; Gu, J.; Yin, A. X.; Zhang, Y. W.; Yan, C. H. Porous Pt-M (M = Cu, Zn, Ni) Nanoparticles as Robust Nanocatalysts. *Chem. Commun.* **2013**, *49* (64), 7168–7170.

90. Wei, Y.; Chen, S.; Lin, Y.; Yang, Z.; Liu, L. Cu-Ag Core-Shell Nanowires for Electronic Skin with a Petal Molded Microstructure. *J. Mater. Chem. C* **2015**, *3* (37), 9594–9602.

91. Mohl, M.; Dobo, D.; Kukovecz, A.; Konya, Z.; Kordas, K.; Wei, J.; Vajtai, R.; Ajayan, P. M. Formation of CuPd and CuPt Bimetallic Nanotubes by Galvanic Replacement Reaction. *J. Phys. Chem. C* **2011**, *115* (19), 9403–9409.

92. Choi, S. Il; Shao, M.; Lu, N.; Ruditskiy, A.; Peng, H. C.; Park, J.; Guerrero, S.; Wang, J.; Kim, M. J.; Xia, Y. Synthesis and Characterization of Pd@Pt-Ni Core-Shell Octahedra with High Activity toward Oxygen Reduction. *ACS Nano* **2014**, *8* (10), 10363–10371.

93. Liu, J.; Chen, B.; Kou, Y.; Liu, Z.; Chen, X.; Li, Y.; Deng, Y.; Han, X.; Hu, W.; Zhong, C. Pt-Decorated Highly Porous Flower-like Ni Particles with High Mass Activity for Ammonia Electro-Oxidation. *J. Mater. Chem. A* **2016**, *4* (28), 11060–11068.

94. Wu, Y.; Wang, D.; Niu, Z.; Chen, P.; Zhou, G.; Li, Y. A Strategy for Designing a Concave Pt-Ni Alloy through Controllable Chemical Etching. *Angew. Chemie - Int. Ed.* **2012**, *51* (50), 12524–12528.

95. Hu, Y.; Wu, P.; Zhang, H.; Cai, C. Synthesis of Graphene-Supported Hollow Pt-Ni Nanocatalysts for Highly Active Electrocatalysis toward the Methanol Oxidation Reaction. *Electrochim. Acta* **2012**, *85*, 314–321.

96. Goris, B.; Polavarapu, L.; Bals, S.; Van Tendeloo, G.; Liz-Marzán, L. M. Monitoring Galvanic Replacement through Three-Dimensional Morphological and Chemical Mapping. *Nano Lett.* **2014**, *14* (6), 3220–3226.

97. Ma, L.; Zhou, X.; Zhang, B.; Bai, Z.; Zhang, Y.; Yuan, Z.; Song, Y.; Yang, K.; Yan, Z.; Han, X. Spiral Silver Nanobelts by Galvanic Replacement. *Mater. Lett.* **2018**, *211*, 312–315.

98. Thota, S.; Chen, S.; Zhao, J. An Unconventional Mechanism of Hollow Nanorod Formation: Asymmetric Cu Diffusion in Au-Cu Alloy Nanorods during Galvanic Replacement Reaction. *Chem. Commun.* **2016**, *52* (32), 5593–5596.

99. Zhang, H.; Jin, M.; Wang, J.; Li, W.; Camargo, P. H. C.; Kim, M. J.; Yang, D.; Xie, Z.; Xia, Y. Synthesis of Pd-Pt Bimetallic Nanocrystals with a Concave Structure through a Bromide-Induced Galvanic Replacement Reaction. *J. Am. Chem. Soc.* **2011**, *133* (15), 6078–6089.

100. Teng, X.; Wang, Q.; Liu, P.; Han, W.; Frenkel, A. I.; Wen, W.; Marinkovic, N.; Hanson, J. C.; Rodriguez, J. A. Formation of Pd/Au Nanostructures from Pd Nanowires via Galvanic Replacement Reaction. *J. Am. Chem. Soc.* **2008**, *130* (3), 1093–1101.

101. El Mel, A. A.; Chettab, M.; Gautron, E.; Chauvin, A.; Humbert, B.; Mevellec, J. Y.; Delacote, C.; Thiry, D.; Stephant, N.; Ding, J.; et al. Galvanic Replacement Reaction: A Route to Highly Ordered Bimetallic Nanotubes. *J. Phys. Chem. C* **2016**, *120* (31), 17652–17659.

102. Au, L.; Lu, X.; Xia, Y. A Comparative Study of Galvanic Replacement Reactions Involving Ag Nanocubes and AuCl2- or AuCl4-. *Adv. Mater.* **2008**, *20* (13), 2517–2522.

103. Sau, T. K.; Rogach, A. L. Nonspherical Noble Metal Nanoparticles: Colloid-Chemical Synthesis and Morphology Control. *Adv. Mater.* **2010**, *22* (16), 1781–1804.

104. Lee, K. E.; Hesketh, A. V.; Kelly, T. L. Chemical Stability and Degradation Mechanisms of Triangular Ag, Ag@Au, and Au Nanoprisms. *Phys. Chem. Chem. Phys.* **2014**, *16* (24), 12407–12414.

105. Collins, G.; McCarty, E. K.; Holmes, J. D. Controlling Alloy Formation and Optical Properties by Galvanic Replacement of Sub-20 Nm Silver Nanoparticles in Organic Media. *CrystEngComm* **2015**, *17* (36), 6999–7005.

106. Gatemala, H.; Ekgasit, S.; Pienpinijtham, P. 3D Structure-Preserving Galvanic Replacement to Create Hollow Au Microstructures. *CrystEngComm* **2017**, *19* (27), 3808–3816.

107. Zheng, F.; Luk, S. Y.; Kwong, T. L.; Yung, K. F. Synthesis of Hollow PtAg Alloy Nanospheres with Excellent Electrocatalytic Performances towards Methanol and Formic Acid Oxidations. *RSC Adv.* **2016**, *6* (50), 44902–44907.

108. Lu, X.; Tuan, H. Y.; Chen, J.; Li, Z. Y.; Korgel, B. A.; Xia, Y. Mechanistic Studies on the Galvanic Replacement Reaction between Multiply Twinned Particles of Ag and HAuCl4 in an Organic Medium. *J. Am. Chem. Soc.* **2007**, *129* (6), 1733–1742.

109. Si, G.; Ma, Z.; Li, K.; Shi, W. Triangular Au-Ag Nanoframes with Tunable Surface Plasmon Resonance Signal from Visible to Near-Infrared Region. *Plasmonics* **2011**, *6* (2), 241–244.

110. Mahmoud, M. A.; Narayanan, R.; El-Sayed, M. A. Enhancing Colloidal Metallic Nanocatalysis: Sharp Edges and Corners for Solid Nanoparticles and Cage Effect for Hollow Ones. *Acc. Chem. Res.* **2013**, *46* (8), 1795–1805.

111. Liaw, J. W.; Cheng, J. C.; Ma, C.; Zhang, R. Theoretical Analysis of Plasmon Modes of Au-Ag Nanocages. *J. Phys. Chem. C* **2013**, *117* (38), 19586–19592.

112. Genç, A.; Patarroyo, J.; Sancho-Parramon, J.; Arenal, R.; Duchamp, M.; Gonzalez, E. E.; Henrard, L.; Bastús, N. G.; Dunin-Borkowski, R. E.; Puntes, V. F.; et al. Tuning the Plasmonic Response up: Hollow Cuboid Metal Nanostructures. *ACS Photonics* **2016**, *3* (5), 770–779.

113. Prieto, M.; Arenal, R.; Henrard, L.; Gomez, L.; Sebastian, V.; Arruebo, M. Morphological Tunability of the Plasmonic Response: From Hollow Gold Nanoparticles to Gold Nanorings. *J. Phys. Chem. C* **2014**, *118* (49), 28804–28811.

114. Genç, A.; Patarroyo, J.; Sancho-Parramon, J.; Bastús, N. G.; Puntes, V.; Arbiol, J. Hollow Metal Nanostructures for Enhanced Plasmonics: Synthesis, Local Plasmonic Properties and Applications. *Nanophotonics* **2017**, *6* (1), 193–213.

115. Si, K. J.; Sikdar, D.; Chen, Y.; Eftekhari, F.; Xu, Z.; Tang, Y.; Xiong, W.; Guo, P.; Zhang, S.; Lu, Y.; et al. Giant Plasmene Nanosheets, Nanoribbons, and Origami. *ACS Nano* **2014**, *8* (11), 11086–11093.

116. Mahmoud, M. A.; Garlyyev, B.; El-Sayed, M. A. Determining the Mechanism of Solution Metallic Nanocatalysis with Solid and Hollow Nanoparticles: Homogeneous or Heterogeneous. *J. Phys. Chem. C* **2013**, *117* (42), 21886–21893.

117. Wang, W.; Yan, Y.; Zhou, N.; Zhang, H.; Li, D.; Yang, D. Seed-Mediated Growth of Au Nanorings with Size Control on Pd Ultrathin Nanosheets and Their Tunable Surface Plasmonic Properties. *Nanoscale* **2016**, *8* (6), 3704–3710.

118. Xiong, W.; Mazid, R.; Yap, L. W.; Li, X.; Cheng, W. Plasmonic Caged Gold Nanorods for Near-Infrared Light Controlled Drug Delivery. *Nanoscale* **2014**, *6* (23), 14388–14393.

119. Meeker, D. G.; Jenkins, S. V.; Miller, E. K.; Beenken, K. E.; Loughran, A. J.; Powless, A.; Muldoon, T. J.; Galanzha, E. I.; Zharov, V. P.; Smeltzer, M. S.; et al. Synergistic Photothermal and Antibiotic Killing of Biofilm-Associated Staphylococcus Aureus Using Targeted Antibiotic-Loaded Gold Nanoconstructs. *ACS Infect. Dis.* **2016**, *2* (4), 241–250.

120. Wang, W.; Tang, Q.; Yu, T.; Li, X.; Gao, Y.; Li, J.; Liu, Y.; Rong, L.; Wang, Z.; Sun, H.; et al. Surfactant-Free Preparation of Au@Resveratrol Hollow Nanoparticles with Photothermal Performance and Antioxidant Activity. *ACS Appl. Mater. Interfaces* **2017**, *9* (4), 3376–3387.

121. Jiang, T.; Song, J.; Zhang, W.; Wang, H.; Li, X.; Xia, R.; Zhu, L.; Xu, X. Au-Ag@Au Hollow Nanostructure with Enhanced Chemical Stability and Improved Photothermal Transduction Efficiency for Cancer Treatment. *ACS Appl. Mater. Interfaces* **2015**, *7* (39), 21985–21994.

122. Cheng, H.; Huo, D.; Zhu, C.; Shen, S.; Wang, W.; Li, H.; Zhu, Z.; Xia, Y. Combination Cancer Treatment through Photothermally Controlled Release of Selenous Acid from Gold Nanocages. *Biomaterials* **2018**, 1–10.

123. Li, N.; Zhao, P.; Astruc, D. Anisotropic Gold Nanoparticles: Synthesis, Properties, Applications, and Toxicity. *Angew. Chemie - Int. Ed.* **2014**, *53* (7), 1756–1789.

124. Ahmad, R.; Fu, J.; He, N.; Li, S. Advanced Gold Nanomaterials for Photothermal Therapy of Cancer. *J. Nanosci. Nanotechnol.* **2016**, *16* (1), 67–80.

125. Shi, P.; Li, M.; Ren, J.; Qu, X. Gold Nanocage-Based Dual Responsive "Caged Metal Chelator" Release System: Noninvasive Remote Control with near Infrared for Potential Treatment of Alzheimer's Disease. *Adv. Funct. Mater.* **2013**, *23* (43), 5412–5419.

126. Lopatynskyi, A. M.; Malymon, Y. O.; Lytvyn, V. K.; Mogylnyi, I. V.; Rachkov, A. E.; Soldatkin, A. P.; Chegel, V. I. Solid and Hollow Gold Nanostructures for Nanomedicine: Comparison of Photothermal Properties. *Plasmonics* **2017**, 1–11.

127. Lin, Z. W.; Tsao, Y. C.; Yang, M. Y.; Huang, M. H. Seed-Mediated Growth of Silver Nanocubes in Aqueous Solution with Tunable Size and Their Conversion to Au Nanocages with Efficient Photothermal Property. *Chem. - A Eur. J.* **2016**, *22* (7), 2326–2332.

128. Huang, S.; Duan, S.; Wang, J.; Bao, S.; Qiu, X.; Li, C.; Liu, Y.; Yan, L.; Zhang, Z.; Hu, Y. Folic-Acid-Mediated Functionalized Gold Nanocages for Targeted Delivery of Anti-MiR-181b in Combination of Gene Therapy and Photothermal Therapy against Hepatocellular Carcinoma. *Adv. Funct. Mater.* **2016**, *26* (15), 2532–2544.

129. Guerrero, A. R.; Hassan, N.; Escobar, C. A.; Albericio, F.; Kogan, M. J.; Araya, E. Gold Nanoparticles for Photothermally Controlled Drug Release. *Nanomedicine (Lond).* **2014**, *9* (13), 2023–2039.

130. Yang, J.; Shen, D.; Zhou, L.; Li, W.; Li, X.; Yao, C.; Wang, R.; El-Toni, A. M.; Zhang, F.; Zhao, D. Spatially Confined Fabrication of Core-Shell Gold Nanocages@Mesoporous Silica for near-Infrared Controlled Photothermal Drug Release. *Chem. Mater.* **2013**, *25* (15), 3030–3037.

131. Xue, W.; Luo, L.; Li, Y.; Yin, T.; Bian, K.; Zhu, R.; Gao, D. Fabrication of Gold Nanocages and Nanoshells Using Lanreotide Acetate and a Comparison Study of Their Photothermal Antitumor Therapy. *J. Mater. Chem. B* **2017**, *5* (28), 5641–5647.

132. Cheemalapati, S.; Ladanov, M.; Pang, B.; Yuan, Y.; Koria, P.; Xia, Y.; Pyayt, A. Dynamic Visualization of Photothermal Heating by Gold Nanocages Using Thermoresponsive Elastin like Polypeptides. *Nanoscale* **2016**, *8* (45), 18912–18920.

133. Jaque, D.; Martínez Maestro, L.; Del Rosal, B.; Haro-Gonzalez, P.; Benayas, A.; Plaza, J. L.; Martín Rodríguez, E.; García Solé, J. Nanoparticles for Photothermal Therapies. *Nanoscale* **2014**, *6* (16), 9494–9530.

134. Srivatsan, A.; Jenkins, S. V.; Jeon, M.; Wu, Z.; Kim, C.; Chen, J.; Pandey, R. K. Gold Nanocage-Photosensitizer Conjugates for Dual-Modal Image-Guided Enhanced Photodynamic Therapy. *Theranostics* **2014**, *4* (2), 163–174.

135. Riley, R. S.; Day, E. S. Gold Nanoparticle-Mediated Photothermal Therapy: Applications and Opportunities for Multimodal Cancer Treatment. *Wiley Interdiscip. Rev. Nanomedicine Nanobiotechnology* **2017**, *9* (4).

136. Rengan, A. K.; Kundu, G.; Banerjee, R.; Srivastava, R. Gold Nanocages as Effective Photothermal Transducers in Killing Highly Tumorigenic Cancer Cells. *Part. Part. Syst. Charact.* **2014**, *31* (3), 398–405.

137. Piao, J. G.; Gao, F.; Li, Y.; Yu, L.; Liu, D.; Tan, Z. Bin; Xiong, Y.; Yang, L.; You, Y. Z. PH-Sensitive Zwitterionic Coating of Gold Nanocages Improves Tumor Targeting and Photothermal Treatment Efficacy. *Nano Res.* **2018**, *11* (6), 3193–3204.

138. Wang, Y.; Black, K. C. L.; Luehmann, H.; Li, W.; Zhang, Y.; Cai, X.; Wan, D.; Liu, S. Y.; Li, M.; Kim, P.; et al. Comparison Study of Gold Nanohexapods, Nanorods, and Nanocages for Photothermal Cancer Treatment. *ACS Nano* **2013**, *7* (3), 2068–2077.

139. Liang, H.; Tian, H.; Deng, M.; Chen, X. Gold Nanoparticles for Cancer Theranostics. *Chinese J. Chem.* **2015**, *33* (9), 1001–1010.

140. Han, J.; Li, J.; Jia, W.; Yao, L.; Li, X.; Jiang, L.; Tian, Y. Photothermal Therapy of Cancer Cells Using Novel Hollow Gold Nanoflowers. *Int. J. Nanomedicine* **2014**, *9* (1), 517–526.

141. Jang, W. D.; Yim, D.; Hwang, I. H. Photofunctional Hollow Nanocapsules for Biomedical Applications. *J. Mater. Chem. B* **2014**, *2* (16), 2202–2211.

142. Dong, L.; Li, Y.; Li, Z.; Xu, N.; Liu, P.; Du, H.; Zhang, Y.; Huang, Y.; Zhu, J.; Ren, G.; et al. Au Nanocage-Strengthened Dissolving Microneedles for Chemo-Photothermal Combined Therapy of Superficial Skin Tumors. *ACS Appl. Mater. Interfaces* **2018**, *10* (11), 9247–9256.

143. Wang, X. Q.; Gao, F.; Zhang, X. Z. Initiator-Loaded Gold Nanocages as a Light-Induced Free-Radical Generator for Cancer Therapy. *Angew. Chemie - Int. Ed.* **2017**, *56* (31), 9029–9033.

144. Ye, X.; Shi, H.; He, X.; Wang, K.; Li, D.; Qiu, P. Gold Nanorod-Seeded Synthesis of Au@Ag/Au Nanospheres with Broad and Intense near-Infrared Absorption for Photothermal Cancer Therapy. *J. Mater. Chem. B* **2014**, *2* (23), 3667–3673.

145. Sanchez-Gaytan, B. L.; Qian, Z.; Hastings, S. P.; Reca, M. L.; Fakhraai, Z.; Park, S. J. Controlling the Topography and Surface Plasmon Resonance of Gold Nanoshells by a Templated Surfactant-Assisted Seed Growth Method. *J. Phys. Chem. C* **2013**, *117* (17), 8916–8923.

146. Pedireddy, S.; Li, A.; Bosman, M.; Phang, I. Y.; Li, S.; Ling, X. Y. Synthesis of Spiky Ag-Au Octahedral Nanoparticles and Their Tunable Optical Properties. *J. Phys. Chem. C* **2013**, *117* (32), 16640–16649.

147. Chien, Y. H.; Tsai, M. F.; Shanmugam, V.; Sardar, K.; Huang, C. L.; Yeh, C. S. Escape from the Destruction of the Galvanic Replacement Reaction for Solid → Hollow → Solid Conversion Process in One Pot Reaction. *Nanoscale* **2013**, *5* (9), 3863–3871.

148. Goodman, A. M.; Cao, Y.; Urban, C.; Neumann, O.; Ayala-Orozco, C.; Knight, M. W.; Joshi, A.; Nordlander, P.; Halas, N. J. The Surprising in Vivo Instability of Near-IR-Absorbing Hollow Au-Ag Nanoshells. *ACS Nano* **2014**, *8* (4), 3222–3231.

149. Wojtysiak, S.; Solla-Gullón, J.; Dłuzewski, P.; Kudelski, A. Synthesis of Core-Shell Silver-Platinum Nanoparticles, Improving Shell Integrity. *Colloids Surfaces A Physicochem. Eng. Asp.* **2014**, *441*, 178–183.

150. Jang, H.; Kim, Y.-K.; Huh, H.; Min, D.-H. Facile Synthesis and Intraparticle Self-Catalytic Oxidation of Dextran-Coated Hollow Au-Ag Nanoshell and Its Application for Chemo-Thermotherapy. *ACS Nano*

2014, *8* (1).

151. Bai, T.; Tan, Y.; Zou, J.; Nie, M.; Guo, Z.; Lu, X.; Gu, N. AuBr2--Engaged Galvanic Replacement for Citrate-Capped Au-Ag Alloy Nanostructures and Their Solution-Based Surface-Enhanced Raman Scattering Activity. *J. Phys. Chem. C* **2015**, *119* (51), 28597–28604.
152. Jabeen, F.; Najam-ul-Haq, M.; Javeed, R.; Huck, C. W.; Bonn, G. K. Au-Nanomaterials as a Superior Choice for near-Infrared Photothermal Therapy. *Molecules* **2014**, *19* (12), 20580–20593.
153. Kang, H.; Jeong, S.; Park, Y.; Yim, J.; Jun, B. H.; Kyeong, S.; Yang, J. K.; Kim, G.; Hong, S.; Lee, L. P.; et al. Near-Infrared SERS Nanoprobes with Plasmonic Au/Ag Hollow-Shell Assemblies for in Vivo Multiplex Detection. *Adv. Funct. Mater.* **2013**, *23* (30), 3719–3727.
154. Soulé, S.; Allouche, J.; Dupin, J. C.; Martinez, H. Design of Ag-Au Nanoshell Core/Mesoporous Oriented Silica Shell Nanoparticles through a Sol-Gel Surfactant Templating Method. *Microporous Mesoporous Mater.* **2013**, *171*, 72–77.
155. Zoppi, A.; Trigari, S.; Giorgetti, E.; Muniz-Miranda, M.; Alloisio, M.; Demartini, A.; Dellepiane, G.; Thea, S.; Dobrikov, G.; Timtcheva, I. Functionalized Au/Ag Nanocages as a Novel Fluorescence and SERS Dual Probe for Sensing. *J. Colloid Interface Sci.* **2013**, *407*, 89–94.
156. Ye, S.; Marston, G.; McLaughlan, J. R.; Sigle, D. O.; Ingram, N.; Freear, S.; Baumberg, J. J.; Bushby, R. J.; Markham, A. F.; Critchley, K.; et al. Engineering Gold Nanotubes with Controlled Length and Near-Infrared Absorption for Theranostic Applications. *Adv. Funct. Mater.* **2015**, *25* (14), 2117–2127.
157. Xiong, W.; Sikdar, D.; Yap, L. W.; Guo, P.; Premaratne, M.; Li, X.; Cheng, W. Matryoshka-Caged Gold Nanorods: Synthesis, Plasmonic Properties, and Catalytic Activity. *Nano Res.* **2016**, *9* (2), 415–423.
158. Wang, Y.; Wen, G.; Ye, L.; Liang, A.; Jiang, Z. Label-Free SERS Study of Galvanic Replacement Reaction on Silver Nanorod Surface and Its Application to Detect Trace Mercury Ion. *Sci. Rep.* **2016**, *6* (October 2015), 1–12.
159. Xiong, W.; Sikdar, D.; Walsh, M.; Si, K. J.; Tang, Y.; Chen, Y.; Mazid, R.; Weyland, M.; Rukhlenko, I. D.; Etheridge, J.; et al. Single-Crystal Caged Gold Nanorods with Tunable Broadband Plasmon Resonances. *Chem. Commun.* **2013**, *49* (83), 9630–9632.
160. Fu, H.; Yang, X.; Jiang, X.; Yu, A. Bimetallic Ag-Au Nanowires: Synthesis, Growth Mechanism, and Catalytic Properties. *Langmuir* **2013**, *29* (23), 7134–7142.

161. Anderson, B. D.; Tracy, J. B. Nanoparticle Conversion Chemistry: Kirkendall Effect, Galvanic Exchange, and Anion Exchange. *Nanoscale* **2014**, *6* (21), 12195–12216.

162. Sun, H.; Guo, X.; Ye, W.; Kou, S.; Yang, J. Charge Transfer Accelerates Galvanic Replacement for PtAgAu Nanotubes with Enhanced Catalytic Activity. *Nano Res.* **2016**, *9* (4), 1173–1181.

163. Jang, H. J.; Ham, S.; Acapulco, J. A. I.; Song, Y.; Hong, S.; Shuford, K. L.; Park, S. Fabrication of 2D Au Nanorings with Pt Framework. *J. Am. Chem. Soc.* **2014**, *136* (50), 17674–17680.

164. Huang, Z.; Raciti, D.; Yu, S.; Zhang, L.; Deng, L.; He, J.; Liu, Y.; Khashab, N. M.; Wang, C.; Gong, J.; et al. Synthesis of Platinum Nanotubes and Nanorings via Simultaneous Metal Alloying and Etching. *J. Am. Chem. Soc.* **2016**, *138* (20), 6332–6335.

165. Gilroy, K. D.; Farzinpour, P.; Sundar, A.; Hughes, R. A.; Neretina, S. Sacrificial Templates for Galvanic Replacement Reactions: Design Criteria for the Synthesis of Pure Pt Nanoshells with a Smooth Surface Morphology. *Chem. Mater.* **2014**, *26* (10), 3340–3347.

166. Lee, S.; Jang, H. J.; Jang, H. Y.; Hong, S.; Moh, S. H.; Park, S. Synthesis and Optical Property Characterization of Elongated AuPt and Pt@Au Metal Nanoframes. *Nanoscale* **2016**, *8* (8), 4491–4494.

167. Zhang, Q.; Guo, X.; Liang, Z.; Zeng, J.; Yang, J.; Liao, S. Hybrid PdAg Alloy-Au Nanorods: Controlled Growth, Optical Properties and Electrochemical Catalysis. *Nano Res.* **2013**, *6* (8), 571–580.

168. Chen, L.; Chabu, J. M.; Liu, Y. Bimetallic AgM (M = Pt, Pd, Au) Nanostructures: Synthesis and Applications for Surface-Enhanced Raman Scattering. *RSC Adv.* **2013**, *3* (13), 4391–4399.

169. Wang, L.; Yamauchi, Y. Metallic Nanocages: Synthesis of Bimetallic Pt-Pd Hollow Nanoparticles with Dendritic Shells by Selective Chemical Etching. *J. Am. Chem. Soc.* **2013**, *135* (45), 16762–16765.

170. Muniz-Miranda, M.; Gellini, C.; Canton, P.; Marsili, P.; Giorgetti, E. SERS and Catalytically Active Ag/Pd Nanoparticles Obtained by Combining Laser Ablation and Galvanic Replacement. *J. Alloys Compd.* **2015**, *615* (S1), S352–S356.

171. Hong, S.; Acapulco, J. A. I.; Jang, H. Y.; Park, S. Au Nanodisk-Core Multishell Nanoparticles: Synthetic Method for Controlling Number of Shells and Intershell Distance. *Chem. Mater.* **2014**, *26*(12), 3618-3623.

172. Wang, X.; Ruditskiy, A.; Xia, Y. Rational Design and Synthesis of Noble-Metal Nanoframes for Catalytic and Photonic Applications. *Natl. Sci. Rev.* **2017**, *3* (4), 520–533.

173. Ham, S.; Jang, H. J.; Song, Y.; Shuford, K. L.; Park, S. Octahedral and Cubic Gold Nanoframes with Platinum Framework. *Angew. Chemie - Int. Ed.* **2015**, *54* (31), 9025–9028.

174. Wang, Z.; Wang, H.; Zhang, Z.; Yang, G.; He, T.; Yin, Y.; Jin, M. Synthesis of Pd Nanoframes by Excavating Solid Nanocrystals for Enhanced Catalytic Properties. *ACS Nano* **2017**, *11* (1), 163–170.

175. Hong, X.; Wang, D.; Cai, S.; Rong, H.; Li, Y. Single-Crystalline Octahedral Au-Ag Nanoframes. *J. Am. Chem. Soc.* **2012**, *134* (44), 18165–18168.

176. Sun, J.; Wang, X.; Liu, J.; Wan, P.; Liao, Q.; Wang, F.; Luo, L.; Sun, X. Highly Stable Ag-Au Nanoplates and Nanoframes for Two-Photon Luminescence. *RSC Adv.* **2014**, *4* (67), 35263–35267.

177. Zhang, L.; Liu, T.; Liu, K.; Han, L.; Yin, Y.; Gao, C. Gold Nanoframes by Nonepitaxial Growth of Au on AgI Nanocrystals for Surface-Enhanced Raman Spectroscopy. *Nano Lett.* **2015**, *15* (7), 4448–4454.

178. Qian, H.; Xu, M.; Li, X.; Ji, M.; Cheng, L.; Shoaib, A.; Liu, J.; Jiang, L.; Zhu, H.; Zhang, J. Surface Micro/Nanostructure Evolution of Au–Ag Alloy Nanoplates: Synthesis, Simulation, Plasmonic Photothermal and Surface-Enhanced Raman Scattering Applications. *Nano Res.* **2016**, *9* (3), 876–885.

179. Fang, Z.; Wang, Y.; Liu, C.; Chen, S.; Sang, W.; Wang, C.; Zeng, J. Rational Design of Metal Nanoframes for Catalysis and Plasmonics. *Small* **2015**, *11* (22), 2593–2605.

180. Tsuji, M.; Kidera, T.; Yajima, A.; Hamasaki, M.; Hattori, M.; Tsuji, T.; Kawazumi, H. Synthesis of Ag-Au and Ag-Pd Alloy Triangular Hollow Nanoframes by Galvanic Replacement Reactions without and with Post-Treatment Using NaCl in an Aqueous Solution. *CrystEngComm* **2014**, *16* (13), 2684–2691.

181. Tsuji, M.; Hamasaki, M.; Yajima, A.; Hattori, M.; Tsuji, T.; Kawazumi, H. Synthesis of Pt-Ag Alloy Triangular Nanoframes by Galvanic Replacement Reactions Followed by Saturated NaCl Treatment in an Aqueous Solution. *Mater. Lett.* **2014**, *121*, 113–117.

182. Lou, Z.; Fujitsuka, M.; Majima, T. Pt-Au Triangular Nanoprisms with Strong Dipole Plasmon Resonance for Hydrogen Generation Studied by Single-Particle Spectroscopy. *ACS Nano* **2016**, *10* (6), 6299–6305.

183. Sung, H. K.; Kim, Y. Synthesis of Au/Ag Nanoframes from Ag Nanoplates by Galvanic Replacement Reaction and Its Optical Properties. *Mater. Lett.* **2015**, *145*, 154–157.

184. Shahjamali, M. M.; Bosman, M.; Cao, S.; Huang, X.; Cao, X.; Zhang, H.; Pramana, S. S.; Xue, C. Surfactant-Free Sub-2 Nm Ultrathin Triangular Gold Nanoframes. *Small* **2013**, *9* (17), 2880–2886.

185. Xu, L.; Luo, Z.; Fan, Z.; Yu, S.; Chen, J.; Liao, Y.; Xue, C. Controllable Galvanic Synthesis of Triangular Ag-Pd Alloy Nanoframes for Efficient Electrocatalytic Methanol Oxidation. *Chem. - A Eur. J.* **2015**, *21* (24), 8691–8695.

186. Qian, H. S.; Guo, H. C.; Ho, P. C. L.; Mahendran, R.; Zhang, Y. Mesoporous-Silica-Coated up-Conversion Fluorescent Nanoparticles for Photodynamic Therapy. *Small* **2009**, *5* (20), 2285–2290.

187. Gao, Y.; Chen, Y.; Ji, X.; He, X.; Yin, Q.; Zhang, Z.; Shi, J.; Li, Y. Controlled Intracellular Release of Doxorubicin in Multidrug-Resistant Cancer Cells by Tuning the Shell-Pore Sizes of Mesoporous Silica Nanoparticles. *ACS Nano* **2011**, *5* (12), 9788–9798.

188. Rosenholm, J. M.; Meinander, a.; Peuhu, E.; Niemi, R.; Eriksson, J. E.; Sahlgren, C.; Lind?n, M. Targeting of Porous Hybrid Silica Nanoparticles to Cancer Cells. *ACS Nano* **2009**, *3* (1), 197–206.

189. Lu, J.; Liong, M.; Zink, J. I.; Tamanoi, F. Mesoporous Silica Nanoparticles as a Delivery System for Hydrophobic Anticancer Drugs. *Small* **2007**, *3* (8), 1341–1346.

190. Lin, Y. S.; Haynes, C. L. Synthesis and Characterization of Biocompatible and Size-Tunable Multifunctional Porous Silica Nanoparticles. *Chem. Mater.* **2009**, *21* (17), 3979–3986.

191. Prabhakar, N.; Näreoja, T.; Von Haartman, E.; Karaman, D. Ş.; Jiang, H.; Koho, S.; Dolenko, T. A.; Hänninen, P. E.; Vlasov, D. I.; Ralchenko, V. G.; et al. Core-Shell Designs of Photoluminescent Nanodiamonds with Porous Silica Coatings for Bioimaging and Drug Delivery II: Application. *Nanoscale* **2013**, *5* (9), 3713–3722.

192. Wu, S.-H.; Mou, C.-Y.; Lin, H.-P. Synthesis of Mesoporous Silica Nanoparticles. *Chem. Soc. Rev.* **2013**, *42* (9), 3862.

193. Nandiyanto, A. B. D.; Kim, S. G.; Iskandar, F.; Okuyama, K. Synthesis of Spherical Mesoporous Silica Nanoparticles with Nanometer-Size Controllable Pores and Outer Diameters. *Microporous Mesoporous Mater.* **2009**, *120* (3), 447–453.

194. Yan, L.; Xu, Y.; Zhou, M.; Chen, G.; Deng, S.; Smirnov, S.; Luo, H.; Zou, G. Porous TiO<inf>2</Inf> Conformal Coating on Carbon Nanotubes as Energy Storage Materials. *Electrochim. Acta* **2015**, *169*, 73–81.

195. Li, H.; Liu, H.; Fu, A.; Wu, G.; Xu, M.; Pang, G.; Guo, P.; Liu, J.; Zhao, X. S. Synthesis and Characterization of N-Doped Porous TiO2hollow Spheres and Their Photocatalytic and Optical Properties. *Materials (Basel).* **2016**, *9* (10).

196. Hwang, S. H.; Yun, J.; Jang, J. Multi-Shell Porous TiO2 Hollow Nanoparticles for Enhanced Light Harvesting in Dye-Sensitized Solar Cells. *Adv. Funct. Mater.* **2014**, *24* (48), 7619–7626.

197. Luo, W.; Wang, Y.; Wang, L.; Jiang, W.; Chou, S.-L.; Dou, S. X.; Liu, H. K.; Yang, J. Silicon/Mesoporous Carbon/Crystalline TiO 2 Nanoparticles for Highly Stable Lithium Storage. *ACS Nano* **2016**, *10* (11), 10524–10532.

198. Cai, Y.; Wang, H. E.; Zhao, X.; Huang, F.; Wang, C.; Deng, Z.; Li, Y.; Cao, G.; Su, B. L. Walnut-like Porous Core/Shell TiO2with Hybridized Phases Enabling Fast and Stable Lithium Storage. *ACS Appl. Mater. Interfaces* **2017**, *9* (12), 10652–10663.

199. Liu, H.; Ji, S.; Zheng, Y.; Li, M.; Yang, H. Porous TiO2-Coated Magnetic Core-Shell Nanocomposites: Preparation and Enhanced Photocatalytic Activity. *Chinese J. Chem. Eng.* **2013**, *21* (5), 569–576.

200. Chen, J. F.; Ding, H. M.; Wang, J. X.; Shao, L. Preparation and Characterization of Porous Hollow Silica Nanoparticles for Drug Delivery Application. *Biomaterials* **2004**, *25* (4), 723–727.

201. Lu, Y.; Jiang, Y.; Chen, W. PtPd Porous Nanorods with Enhanced Electrocatalytic Activity and Durability for Oxygen Reduction Reaction. *Nano Energy* **2013**, *2* (5), 836–844.

202. Guo, Y.; Xu, Y. T.; Gao, G. H.; Wang, T.; Zhao, B.; Fu, X. Z.; Sun, R.; Wong, C. P. Electro-Oxidation of Formaldehyde and Methanol over Hollow Porous Palladium Nanoparticles with Enhanced Catalytic Activity. *Catal. Commun.* **2015**, *58*, 40–45.

203. Malgras, V.; Ataee-Esfahani, H.; Wang, H.; Jiang, B.; Li, C.; Wu, K. C. W.; Kim, J. H.; Yamauchi, Y. Nanoarchitectures for Mesoporous Metals. *Adv. Mater.* **2016**, *28* (6), 993–1010.

204. Li, X.; Chen, Q.; McCue, I.; Snyder, J.; Crozier, P.; Erlebacher, J.; Sieradzki, K. Dealloying of Noble-Metal Alloy Nanoparticles. *Nano Lett.* **2014**, *14* (5), 2569–2577.

205. Zhang, Q.; Large, N.; Nordlander, P.; Wang, H. Porous Au Nanoparticles with Tunable Plasmon Resonances and Intense Field Enhancements for Single-Particle SERS. *J. Phys. Chem. Lett.* **2014**, *5* (2), 370–374.

206. Jiang, B.; Li, C.; Tang, J.; Takei, T.; Kim, J. H.; Ide, Y.; Henzie, J.; Tominaka, S.; Yamauchi, Y. Tunable-Sized Polymeric Micelles and Their Assembly for the Preparation of Large Mesoporous Platinum Nanoparticles. *Angew. Chemie - Int. Ed.* **2016**, *55* (34), 10037–10041.

207. Fu, G.; Liu, Z.; Chen, Y.; Lin, J.; Tang, Y.; Lu, T. Synthesis and Electrocatalytic Activity of Au@Pd Core-Shell Nanothorns for the Oxygen Reduction Reaction. *Nano Res.* **2014**, *7* (8), 1205–1214.

208. Fu, T.; Fang, J.; Wang, C.; Zhao, J. Hollow Porous Nanoparticles with Pt Skin on a Ag-Pt Alloy Structure as a Highly Active Electrocatalyst for the Oxygen Reduction Reaction. *J. Mater. Chem. A* **2016**, *4* (22), 8803–8811.

209. Li, C.; Yamauchi, Y. Facile Solution Synthesis of Ag@Pt Core-Shell Nanoparticles with Dendritic Pt Shells. *Phys. Chem. Chem. Phys.* **2013**, *15* (10), 3490–3496.

210. Liu, K.; Bai, Y.; Zhang, L.; Yang, Z.; Fan, Q.; Zheng, H.; Yin, Y.; Gao, C. Porous Au-Ag Nanospheres with High-Density and Highly Accessible Hotspots for SERS Analysis. *Nano Lett.* **2016**, *16* (6), 3675–3681.

211. Zhu, C.; Du, D.; Eychmüller, A.; Lin, Y. Engineering Ordered and Nonordered Porous Noble Metal Nanostructures: Synthesis, Assembly, and Their Applications in Electrochemistry. *Chem. Rev.* **2015**, *115* (16), 8896–8943.

212. Jang, H.; Min, D. -H. Spherically-Clustered Porous Au-Ag Nanoparticle Prepared by Partial Inhibition of Galvanic Replacement and Its Application for Efficient Multi-Modal Therapy. *ACS Nano*, **2015**, *9*(3), 2696-2703.

213. Kang, S.; Kang, K.; Huh, H.; Kim, H.; Chang, S. -J.; Park, J. T.; Chang, K. S.; Min, D. -H.; Jang, H. Reducing Agent-Assisted Excessive Galvanic Replacement Mediated Seed-Mediated Synthesis of Porous Gold Nanoplates and Highly Efficient Gene-Thermo Cancer Therapy. *ACS Appl. Mater. Interfaces*, **2017**, *9*(40), 35268-35278.

214. Kumar, P. S.; Pastoriza-santos, I.; Rodr, B.; Liz-marz, L. M. High-Yield Synthesis and Optical Response of Gold Nanostars. **2008**.

215. Ortiz, N.; Skrabalak, S. E. Controlling the Growth Kinetics of Nanocrystals via Galvanic Replacement: Synthesis of Au Tetrapods and Star-Shaped Decahedra. *Cryst. Growth Des.* **2011**, *11* (8), 3545–3550.

216. Ma, T.; Yang, W.; Liu, S.; Zhang, H.; Liang, F. A Comparison Reduction of 4-Nitrophenol by Gold Nanospheres and Gold Nanostars. *Catalysts* **2017**, *7* (2), 38.

217. Cao, X.; Shan, Y.; Tan, L.; Yu, X.; Bao, M.; Li, W.; Shi, H. Hollow Au Nanoflower Substrates for Identification and Discrimination of the Differentiation of Bone Marrow Mesenchymal Stem Cells by Surface-Enhanced Raman Spectroscopy. *J. Mater. Chem. B* **2017**, *5* (30), 5983–5995.

218. Boyne, D. A.; Orlicki, J. A.; Walck, S. D.; Savage, A. M.; Li, T.; Griep, M. H. Plasmonic Gold Nanostars as Optical Nano-Additives for Injection Molded Polymer Composites. *Nanotechnology* **2017**, *28* (40).

219. Xu, M.; Zhang, J. Precisely Controllable Synthesized Nanoparticles for Surface Enhanced Raman Spectroscopy Precisely Controllable Synthesized Nanoparticles for Surface Enhanced Raman Spectroscopy.

220. Paramasivam, G.; Kayambu, N.; Rabel, A. M.; Sundramoorthy, A. K.; Sundaramurthy, A. Anisotropic Noble Metal Nanoparticles: Synthesis, Surface Functionalization and Applications in Biosensing, Bioimaging, Drug Delivery and Theranostics. *Acta Biomater.* **2017**, *49*, 45–65.

221. Wei, Y.; Zhao, Z.; Yang, P. Pd-Tipped Au Nanorods for Plasmon-Enhanced Electrocatalytic Hydrogen Evolution with Photoelectric and Photothermal Effects. *ChemElectroChem* **2018**, *5* (5), 778–784.

222. Zhang, W.; Yang, J.; Lu, X. Tailoring Galvanic Replacement Reaction for the Preparation of Pt/Ag Bimetallic Hollow Nanostructures with Controlled Number of Voids. *ACS Nano* **2012**, *6* (8), 7397–7405.

223. Jang, H.; Kim, Y. K.; Min, D. H. Synthesis of Partially Dextran-Coated Gold Nanoworms and Anisotropic Structure Based Dual-Strategic Cargo Conjugation for Efficient Combinational Cancer Therapy. *Chem. Commun.* **2017**, *53* (8), 1385–1388.

224. Kang, S.; Shin, W.; Kang, K.; Choi, M. H.; Kim, Y. J.; Kim, Y. K.; Min, D. H.; Jang, H. Revisiting of Pd Nanoparticles in Cancer Treatment: All-Round Excellence of Porous Pd Nanoplates in Gene-Thermo Combinational Therapy. *ACS Appl. Mater. Interfaces* **2018**, *10* (16), 13819–13828.

225. Guo, X.; Ye, W.; Zhu, R.; Wang, W.; Xie, F.; Sun, H.; Zhao, Q.; Ding, Y.; Yang, J. Gold Nanorod-Templated Synthesis of Polymetallic Hollow Nanostructures with Enhanced Electrocatalytic Performance. *Nanoscale* **2014**, *6* (20), 11732–11737.

226. Tsuji, M.; Nakashima, Y.; Yajima, A.; Hattori, M. Formation of Rh Frame Nanorods Using Au Nanorods as Sacrificial Templates. *CrystEngComm* **2015**, *17* (36), 6955–6961.

227. Jiang, B.; Kani, K.; Iqbal, M.; Abe, H.; Kimura, T.; Hossain, M. S. A.; Anjaneyulu, O.; Henzie, J.; Yamauchi, Y. Mesoporous Bimetallic RhCu Alloy Nanospheres Using a Sophisticated Soft-Templating Strategy. *Chem. Mater.* **2018**, *30* (2), 428–435.

228. Zhang, Y.; Ahn, J.; Liu, J.; Qin, D. Syntheses, Plasmonic Properties, and Catalytic Applications of Ag-Rh Core-Frame Nanocubes and Rh Nanoboxes with Highly Porous Walls. *Chem. Mater.* **2018**, *30* (6), 2151–2159.

229. Kang, S.; Shin, W.; Choi, M.; Ahn, M.; Kim, Y.-K.; Kim, S.; Min, D.; Jang, H. Morphology-Controlled Synthesis of Rhodium Nanoparticles for Cancer Phototherapy. *ACS Nano* **2018**, acsnano.8b02698.

230. Han, L.; Wang, P.; Liu, H.; Tan, Q.; Yang, J. Balancing the Galvanic Replacement and Reduction Kinetics for the General Formation of Bimetallic CuM (M = Ru, Rh, Pd, Os, Ir, and Pt) Hollow Nanostructures. *J. Mater. Chem. A* **2016**, *4* (47), 18354–18365.

231. Pei, J.; Mao, J.; Liang, X.; Chen, C.; Peng, Q.; Wang, D.; Li, Y. Ir-Cu Nanoframes: One-Pot Synthesis and Efficient Electrocatalysts for Oxygen Evolution Reaction. *Chem. Commun.* **2016**, *52* (19), 3793–3796.

232. Wang, C.; Sui, Y.; Xiao, G.; Yang, X.; Wei, Y.; Zou, G.; Zou, B. Synthesis of Cu-Ir Nanocages with Enhanced Electrocatalytic Activity for the Oxygen Evolution Reaction. *J. Mater. Chem. A* **2015**, *3* (39), 19669–19673.

233. Huang, X.; Chen, Y.; Chiu, C. Y.; Zhang, H.; Xu, Y.; Duan, X.; Huang, Y. A Versatile Strategy to the Selective Synthesis of Cu Nanocrystals and the in Situ Conversion to CuRu Nanotubes. *Nanoscale* **2013**, *5* (14), 6284–6290.

234. Sieben, J. M.; Comignani, V.; Alvarez, A. E.; Duarte, M. M. E. Synthesis and Characterization of Cu Core Pt-Ru Shell Nanoparticles for the Electro-Oxidation of Alcohols. *Int. J. Hydrogen Energy* **2014**, *39* (16), 8667–8674.

235. Chen, Y.; Yu, Z.; Chen, Z.; Shen, R.; Wang, Y.; Cao, X.; Peng, Q.; Li, Y. Controlled One-Pot Synthesis of RuCu Nanocages and Cu@Ru Nanocrystals for the Regioselective Hydrogenation of Quinoline. *Nano Res.* **2016**, *9* (9), 2632–2640.

236. Oh, M. H.; Yu, T.; Yu, S. -H.; Lim, B.; Ko, K. -T.; Willinger, M. -G.; Seo, D. -H.; Kim, B. H.; Cho, M. G.; Park, J. -H.; Kang, K.; Sung, Y. -E.; Pinna, N.; Hyeon, T. Galvanic Replacement Reactions in Metal Oxide Nanocrystals. *Science*, **2013**, *340*, 964-968.

237. Lee, D. G.; Kim, S. M.; Jeong, H.; Kim, J.; Lee, I. S. Surface-Specific Deposition of Catalytic Metal Nanocrystals on Hollow Carbon Nanospheres via Galvanic Replacement Reactions of Carbon-Encapsulated MnO Nanoparticles. *ACS Nano* **2014**, *8* (5), 4510–4521.

238. Huang, Y.; Wei, T.; Yu, J.; Hou, Y.; Cai, K.; Liang, X. J. Multifunctional Metal Rattle-Type Nanocarriers for MRI-Guided Photothermal Cancer Therapy. *Mol. Pharm.* **2014**, *11* (10), 3386–3394.

239. Jeon, S. L.; Chae, M. K.; Jang, E. J.; Lee, C. Cleaved Iron Oxide Nanoparticles as T_2 Contrast Agents for Magnetic Resonance Imaging. *Chem. - A Eur. J.* **2013**, *19* (13), 4217–4222.

240. Pellico, J.; Ruiz-Cabello, J.; Fernández-Barahona, I.; Gutiérrez, L.; Lechuga-Vieco, A. V.; Enríquez, J. A.; Morales, M. P.; Herranz, F. One-Step Fast Synthesis of Nanoparticles for MRI: Coating Chemistry as the Key Variable Determining Positive or Negative Contrast. *Langmuir* **2017**, *33* (39), 10239–10247.

241. López-Ortega, A.; Roca, A. G.; Torruella, P.; Petrecca, M.; Estradé, S.; Peiró, F.; Puntes, V.; Nogués, J. Galvanic Replacement onto Complex Metal-Oxide Nanoparticles: Impact of Water or Other Oxidizers in the Formation of Either Fully Dense Onion-like or Multicomponent Hollow MnOx/FeOxStructures. *Chem. Mater.* **2016**, *28* (21), 8025–8031.

242. Zhao, Z.; Chi, X.; Yang, L.; Yang, R.; Ren, B. W.; Zhu, X.; Zhang, P.; Gao, J. Cation Exchange of Anisotropic-Shaped Magnetite Nanoparticles Generates High-Relaxivity Contrast Agents for Liver Tumor Imaging. *Chem. Mater.* **2016**, *28* (10), 3497–3506.

Preprints (www.preprints.org) | NOT PEER-REVIEWED | Posted: 13 July 2018 doi:10.20944/preprints201807.0226.v1

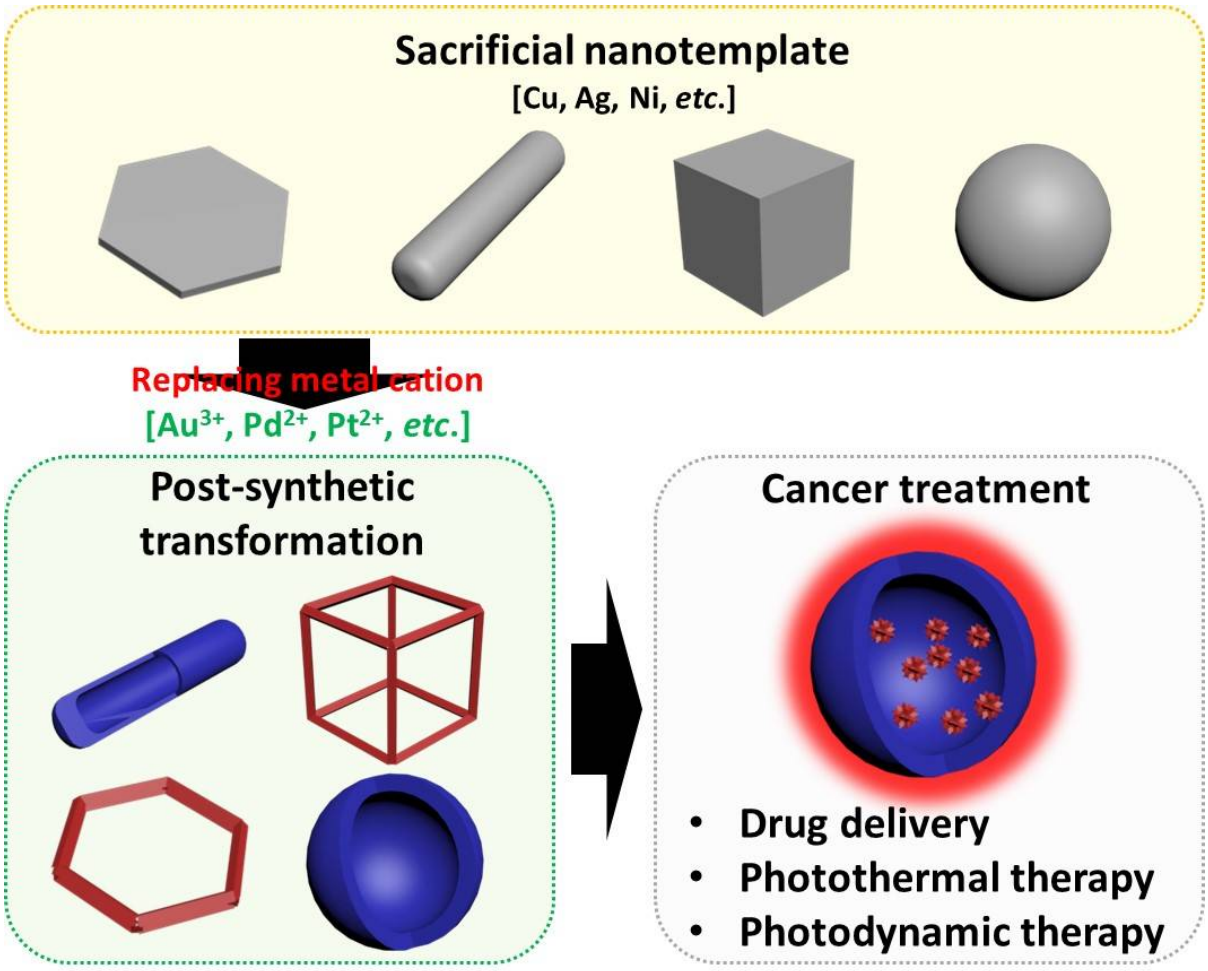

Figure 1. Overall scheme of galvanic replacement mediated post-synthetic transformation of nanoparticles and their potential application in cancer treatment by using advantages in drug delivery, photothermal therapy, and photodynamic therapy.

Preprints (www.preprints.org) | NOT PEER-REVIEWED | Posted: 13 July 2018 doi:10.20944/preprints201807.0226.v1

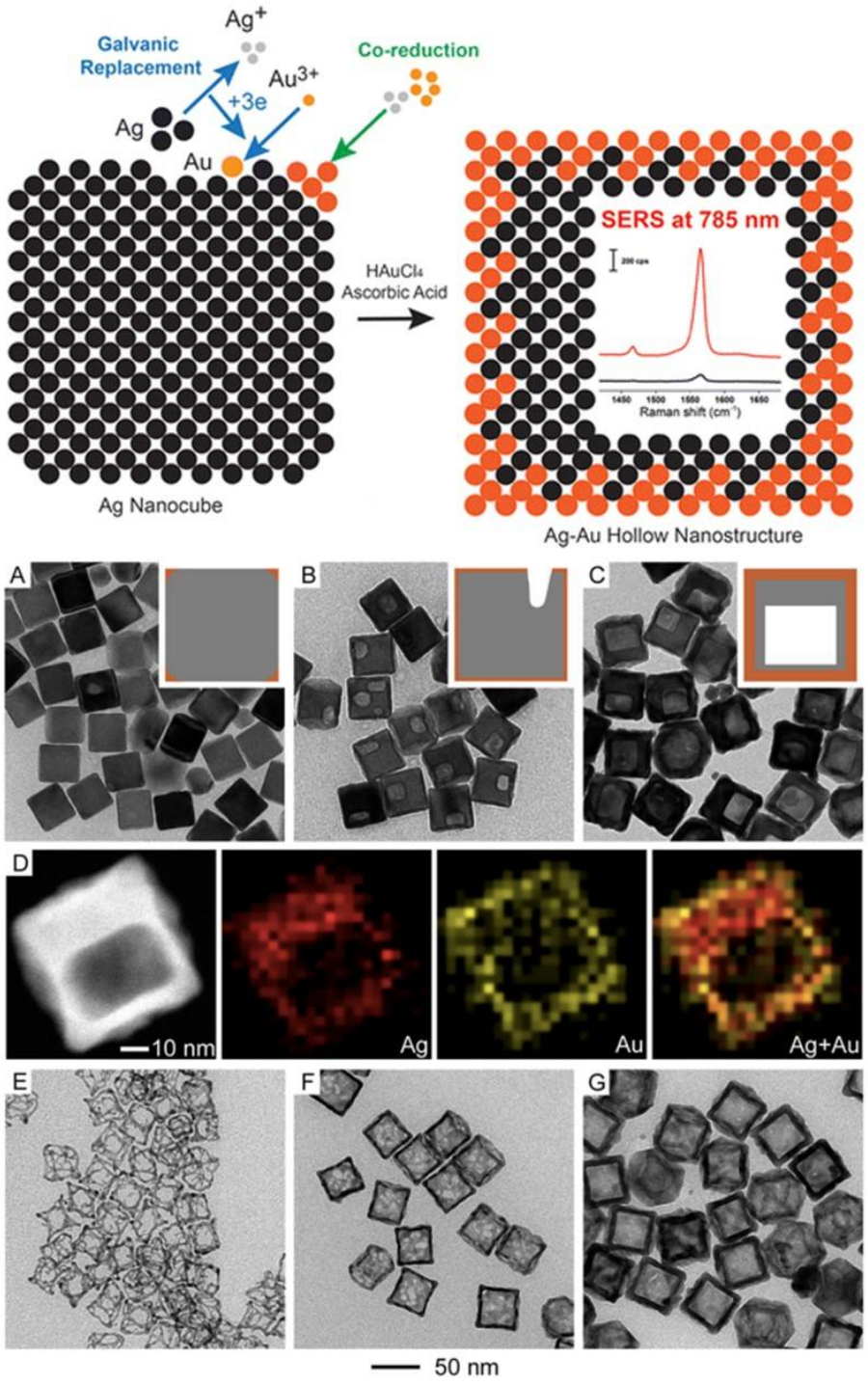

Figure 2. Ag nanocube template based galvanic replacement to manufacture hollow nanocage and nanoframe. Schematic illustration of ascorbic acid assisted galvanic replacement and their potential application in SERS (top). Different volume of replacing Au(III) addition in the presence of ascorbic acid: (A) 0.05, (B) 0.2, and (C) 0.6 mL. (D) HAADF-STEM/EDX mapping of 0.6 mL Au(III) condition. (E-G) TEM images of nanostructures from subsequent etching with H_2O_2. Reprinted with permission from ref.70. Copyright © 2014, American Chemical Society.

Preprints (www.preprints.org) | NOT PEER-REVIEWED | Posted: 13 July 2018 doi:10.20944/preprints201807.0226.v1

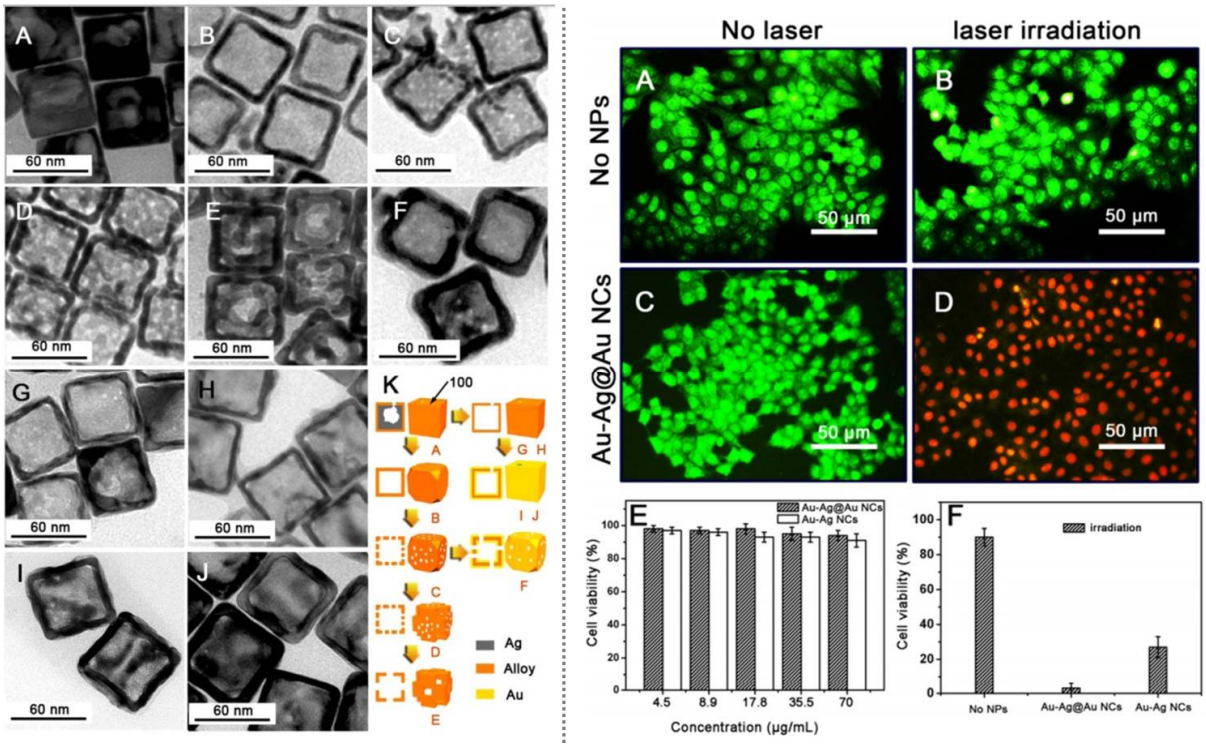

Figure 3. TEM images of Ag nanocubes after reaction with different volumes of Au(III) with their schematic illustration (left from dotted line). Comparison of photothermal destruction of MCF-7 breast cancer cells without (A,B) and with (C,D) the incubation of PEGylated nanoshells. (E) cell viability of MCF-7 cells after incubation with nanoshells and (F) with laser irradiation (right from dotted line). Reprinted with permission from ref.121. Copyright © 2015, American Chemical Society.

Preprints (www.preprints.org) | NOT PEER-REVIEWED | Posted: 13 July 2018 doi:10.20944/preprints201807.0226.v1

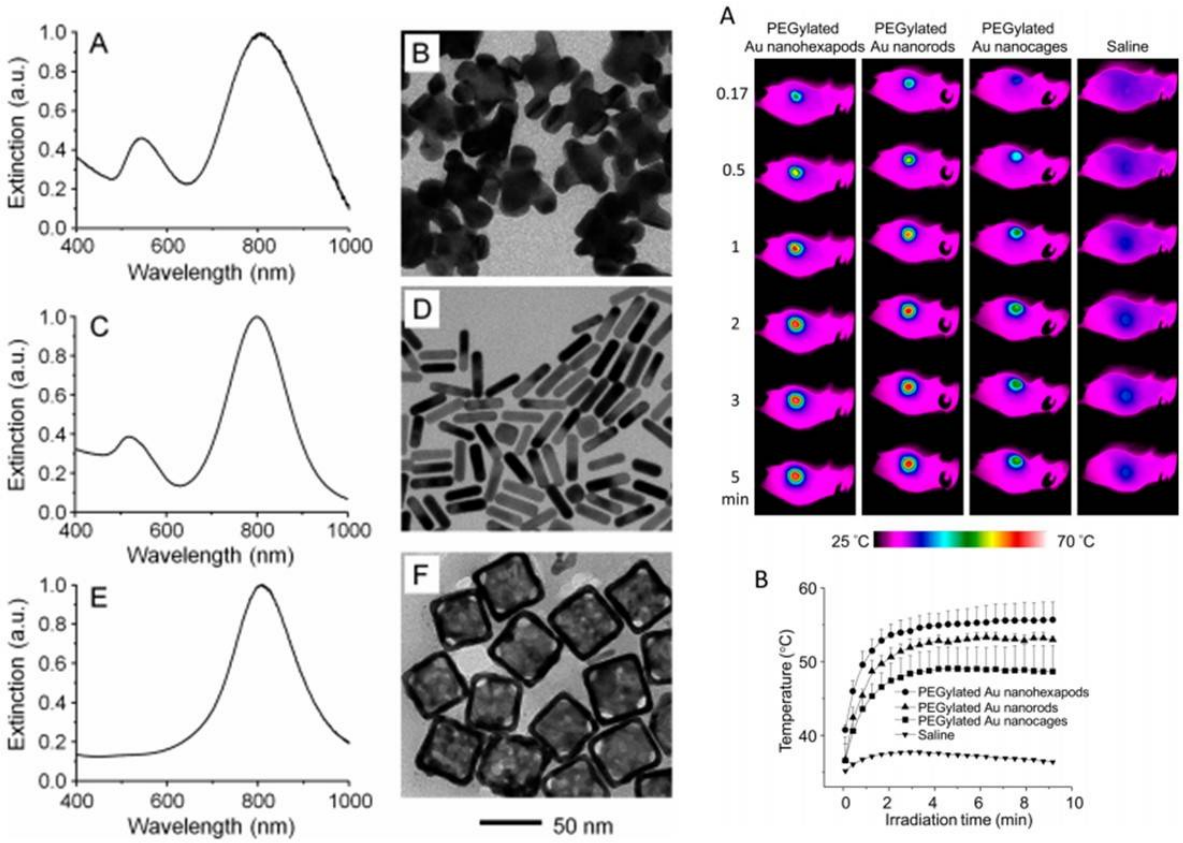

Figure 4. UV-Vis spectra taken from aqueous suspensions of (A) Au nanohexapods, (C) Au nanorods, and (E) Au nanocages with their TEM images (B,D,F), respectively. Thermographs of tumor-bearing mice receiving photothermal treatment for different periods of time with each nanostructures (A, right) and measured temperature elevation (B, right). Reprinted with permission from ref.138. Copyright © 2013, American Chemical Society.

Preprints (www.preprints.org) | NOT PEER-REVIEWED | Posted: 13 July 2018 doi:10.20944/preprints201807.0226.v1

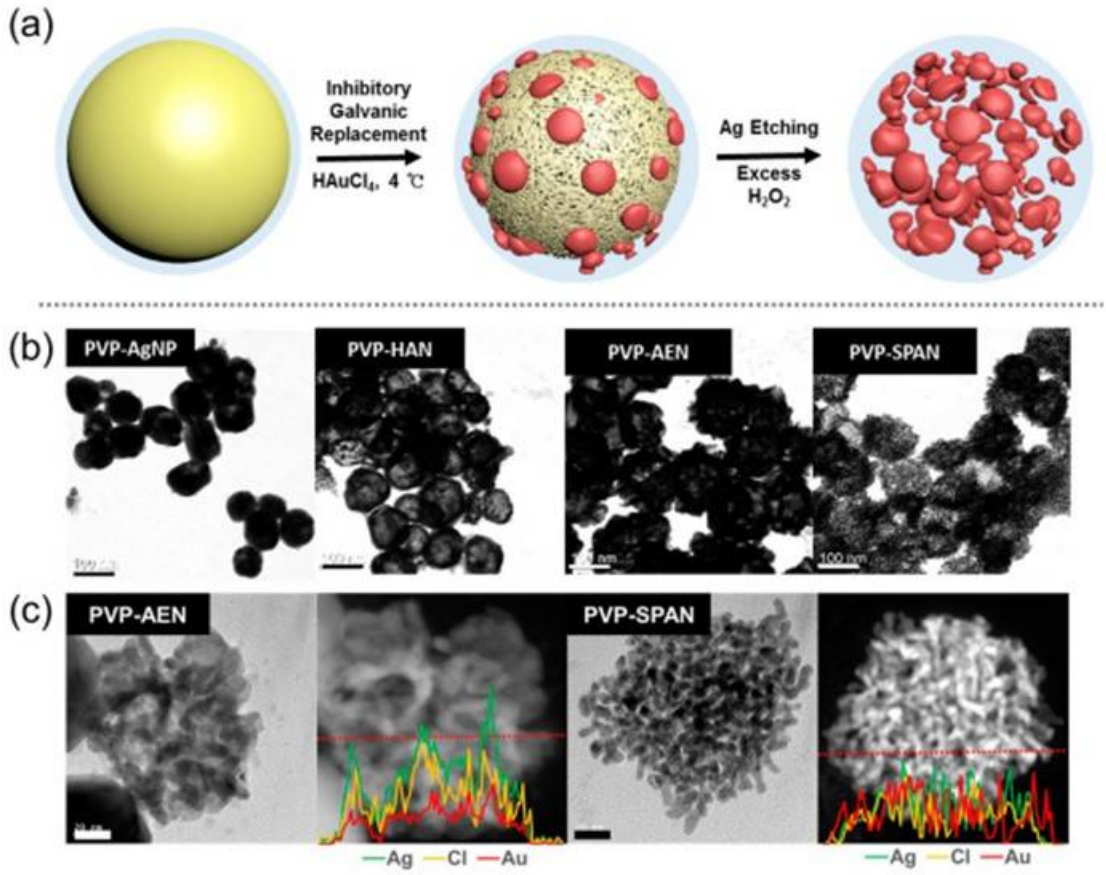

Figure 5. (a) Schematic illustration of porous Au nanoparticle synthesis by inhibitory galvanic replacement with subsequent etching process. (b,c) TEM and HR-TEM images with EDX line profiling. Reprinted with permission from ref.212. Copyright © 2015, American Chemical Society.

Preprints (www.preprints.org) | NOT PEER-REVIEWED | Posted: 13 July 2018 doi:10.20944/preprints201807.0226.v1

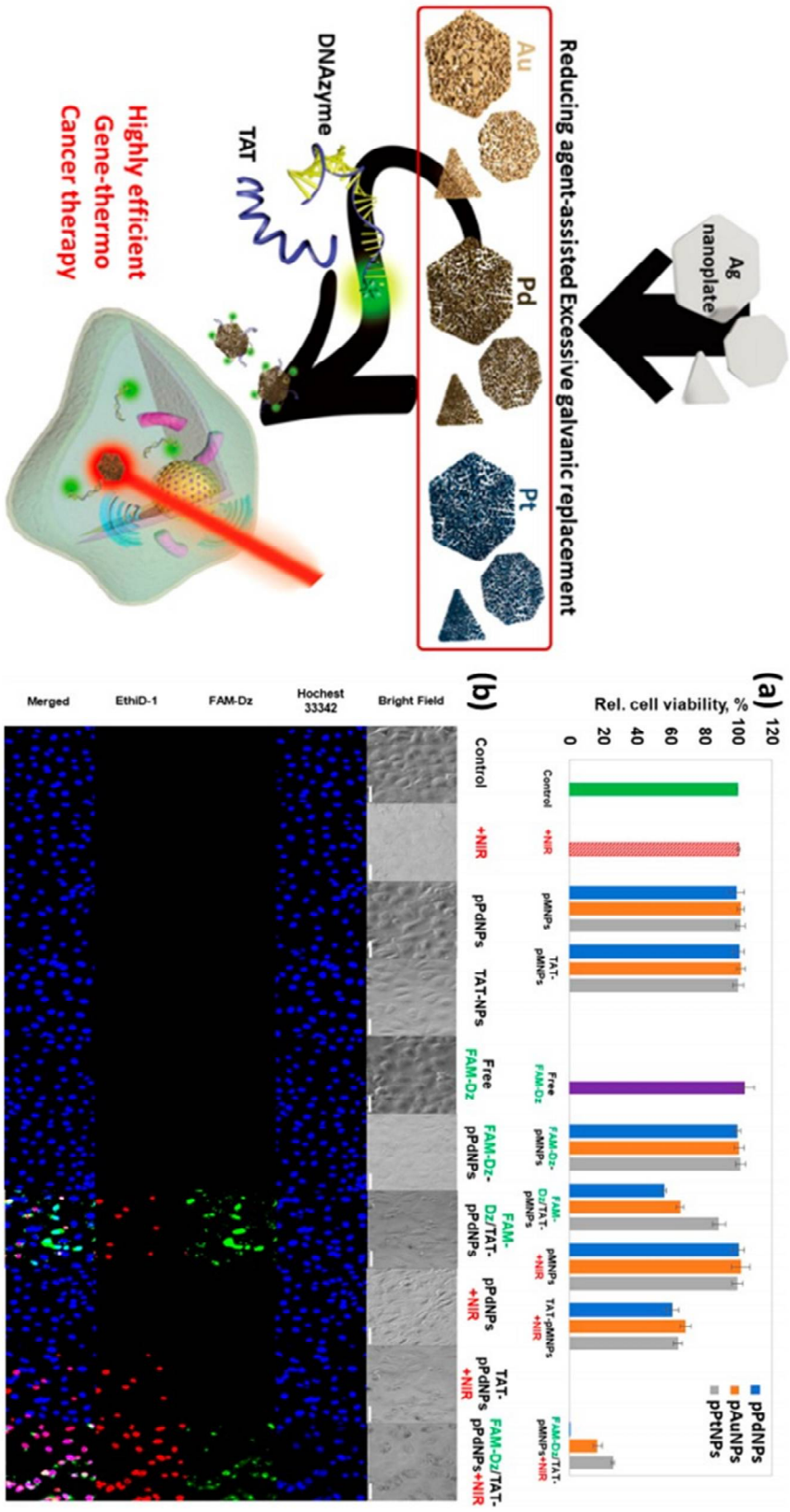

Figure 6. Schematic illustration of porous Au, Pd, and Pt nanoplate synthesis and their efficiency comparison in gene-thermo cancer treatment (top). (a) quantitative gene-thermo cancer treatment efficiency by cell viability

 doi:10.20944/preprints201807.0226.v1

assay and (b) fluorescence microscope image of porous Pd nanoplate mediated cancer treatment. Reprinted with permission from ref.224. Copyright © 2018, American Chemical Society.

Preprints (www.preprints.org) | NOT PEER-REVIEWED | Posted: 13 July 2018 doi:10.20944/preprints201807.0226.v1

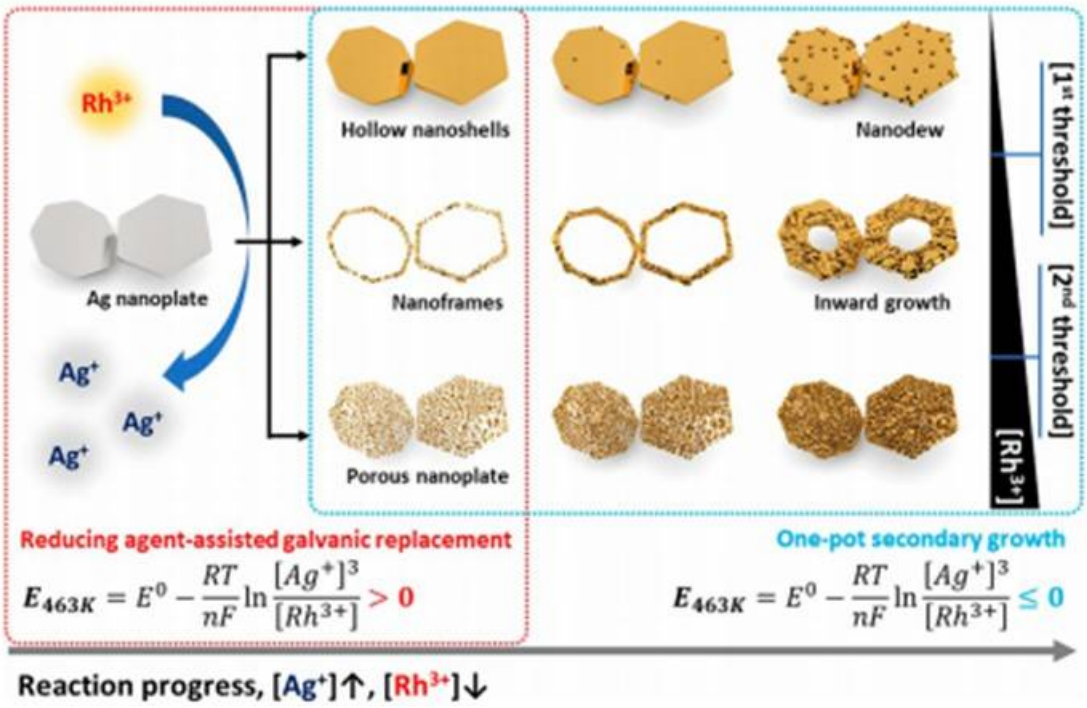

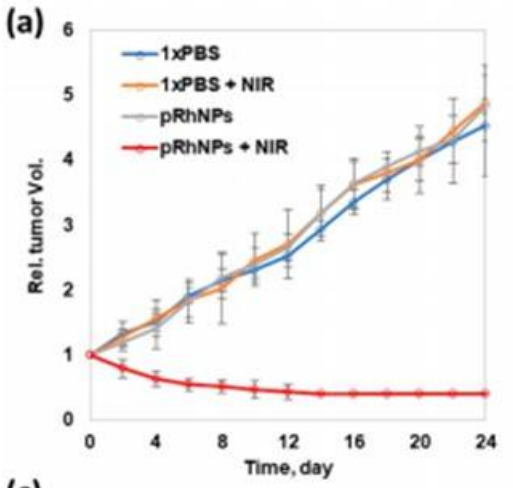

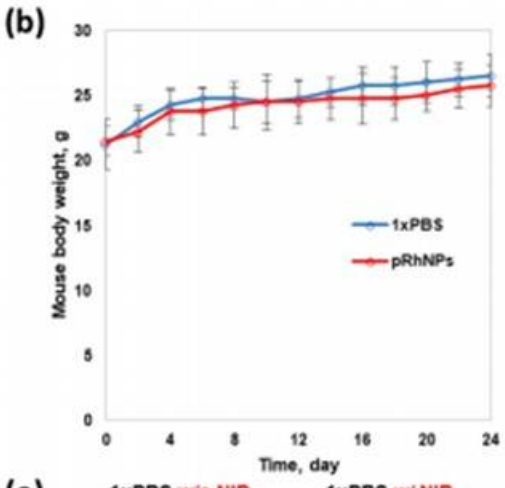

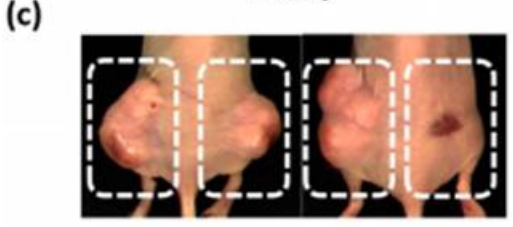

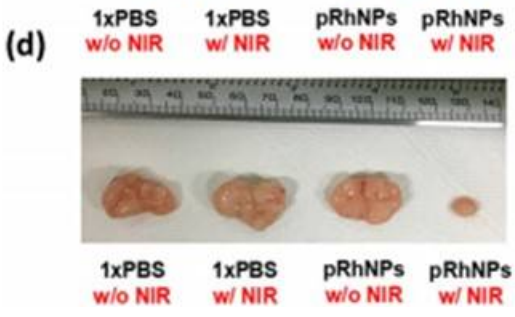

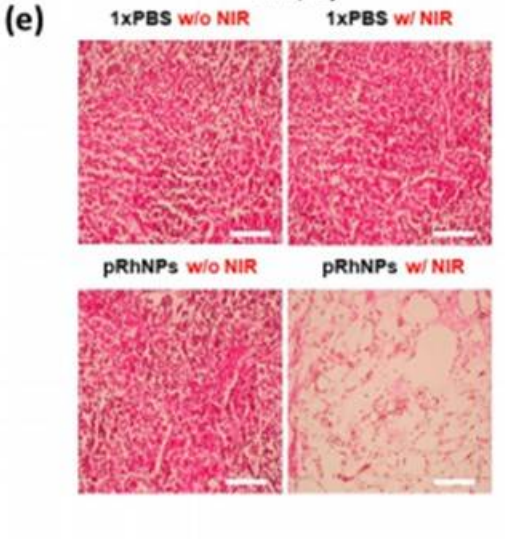

 doi:10.20944/preprints201807.0226.v1

Figure 7. Schematic illustration of hollow Rh nanoshell, Rh nanoframe and porous Rh nanoplate synthesis through inverse directional galvanic replacement (top). (a) in vivo tumor ablation by porous Rh nanoplate with 808 nm NIR laser irradiation with (b) body weight tracking. (c,d) Digital images clearly exhibited the efficient cancer treatment. (e) H&E staining mediated tumor tissue observation. Reprinted with permission from ref.229.